CHAPTER

1

c0001 # Nonsolvent-induced phase separation

Ahmad Rahimpour[1,2], *Mohammadreza Shirzad Kebria*[2], *Mostafa Dadashi Firouzjaei*[3], *Mohammad Mozafari*[2], *Mark Elliott*[3] *and Mohtada Sadrzadeh*[1]

[1]**Department of Mechanical Engineering, 10-367 Donadeo Innovation Center for Engineering, Advanced Water Research Lab (AWRL), University of Alberta, Edmonton, AB, Canada;** [2]**Department of Chemical Engineering, Babol Noshirvani University of Technology, Babol Mazandaran, Iran;** [3]**Department of Civil, Construction and Environmental Engineering, University of Alabama, Tuscaloosa, AL, United States**

s0010 ## 1. Introduction

p0010 Polymeric membranes play a crucial role in separation technologies as they are widely used in various applications, including gas separation, reverse osmosis, ultrafiltration, microfiltration, pervaporation, dialysis, and supported liquid membrane extraction [1–6]. For the integrally skinned asymmetric membranes, the surface pore sizes and their distribution usually determine the separation performance, or selectivity, while the thickness of the selective layer determines the membrane permeability. In the last 4 decades, membrane and material scientists developed advanced materials and improved fabrication methods to create desirable pore structures, thin selective layers, and stable performance during long-term filtration [7–12]. Generally, several fabrication methods, such as stretching, vapor deposition, sintering, sol-gel, solution coating, track-etching, and phase inversion, are used to fabricate membranes, with the latter being the most versatile method due to its simplicity and scalability of the fabrication process [13–17]. Phase inversion technique enables preparing all types of morphologies from a vast number of polymeric materials [18–21]. During the phase inversion process, a homogeneous polymer solution becomes insoluble at a certain condition and separates into two phases: (i) a polymer-rich phase that forms the membrane matrix after solidification and (ii) a polymer-poor phase that creates the membrane pore after exchanging the solvent with nonsolvents followed by drying [15,22]. Several ways can be applied to induce phase separation. These include lowering the cast film temperature in thermally induced phase separation (TIPS) [2], immersion of cast film into a nonsolvent bath in nonsolvent-

Polymeric Membrane Formation by Phase Inversion
https://doi.org/10.1016/B978-0-323-95628-4.00009-4

10001-TAVAJOHI-9780323956284

induced phase separation (NIPS) [3], nonsolvent adsorption from a vapor phase in vapor-induced phase separation (VIPS), and evaporation of a volatile solvent from the casting solution evaporation-induced phase separation (EIPS). Among these phase inversion methods, NIPS (also known as the Loeb-Sourirajan method) is the most widely utilized method to fabricate commercial asymmetric polymeric membranes for various industries and markets [13,23,24]. In the 1960s, Loeb and Sourirajan used the immersion precipitation technique to form an integrally skinned asymmetric membrane. For this purpose, they cast a polymeric film on a substrate and observed its transformation to a solid phase in a controlled manner [25], a breakthrough in membrane separation technology. The formation of asymmetric membranes by the NIPS process consists of a couple of steps: (1) dope preparation, (2) degassing, (3) casting (4), evaporation (optional based on the application), (5) coagulation and solvent exchange, and (6) posttreatment. The membranes fabricated by the NIPS process mostly have a thin, dense, selective skin layer over a thick porous sublayer, which has no significant mass transport resistance against the permeate phase. The skin layer and porous substructure are composed of the same material. The properties of the skin layer, as a separating layer, are one of the major key elements in determining membrane productivity and separation factor for liquid and gas separations. This chapter aims to review the fundamental understanding of the NIPS process and the materials and technology developed for the fabrication of asymmetric membranes with desired characteristics and performance. The basic principles of membrane formation by the NIPS process are provided in the following section.

2. Membrane fabrication by NIPS technique: Principal and basic understanding

p0015 NIPS process is based on separating a homogeneous and one-phase solution, consisting of a polymer, a solvent, and additives, into two distinct phases, that is, the solid or polymer-rich phase and solvent-rich liquid or polymer-lean phase. The former is responsible for forming the membrane matrix, whereas the second phase is washed out during the membrane formation process. This causes the development of pore structure and network within the matrix of the membrane until solidification completes. Generally, NIPS process can be carried out in two ways: by straight plunging a polymer solution into a nonsolvent coagulation bath, which is called the wet method, and by giving time to a polymer solution for solvent evaporation and then plunging it in nonsolvent coagulation bath, known as the dry/wet method. From the mass transfer point of view, a concentration gradient appears across the polymer solution during the membrane preparation procedure due to the solvent evaporation or replacement of solvent and nonsolvent, which leads to asymmetric membranes.

p0020 Several types of membranes such as flat sheet, hollow fiber (diameter <0.5 mm), and capillary (0.5 mm $<$ diameter <5 mm) membranes can be prepared using the NIPS method [13]. Flat sheet membranes are usually formed by coating a thin polymeric layer on the porous substrate. After casting a dope solution, consisting of a polymer or blends of polymers, additives, and solvent(s), on the surface of the substrate, the membrane is immersed into a coagulation bath containing nonsolvent, which is miscible with solvent. After nonsolvent transport to the polymer solution, the dope solution composition moves from the homogenous and thermodynamically stable one-phase region to the metastable or unstable and nonhomogenous two-phase region to conduct phase separation. The phase separation progresses until the

precipitation of the polymer-rich phase is complete, and the porous structure is created. This procedure is used in the laboratory to fabricate small membranes (up to 50 cm long and 30 cm wide) with a blade or casting knife [26–28]. A typical lab-scale hand-held casting knife/blade and procedure of NIPS for membrane fabrication are shown in Fig. 1.1.

p0025 Large casting machines (Fig. 1.2) are used to produce the membrane rolls for commercial production of flat sheet membranes, commonly up to 1000 m long and 1 m wide. Briefly, the polymer casting solution is cast onto a moving nonwoven polyester or polyethylene fabric. The cast film is rolled to immerse in a water bath, as a nonsolvent, to initiate the polymer precipitation. The precipitation starts rapidly on the top surface of the cast film, leading to the formation of a dense and selective skin layer for the membrane. This dense layer reduces the water penetration rate into the underlying cast polymer film, which slows the polymer precipitation at this layer considerably, leading to a more porous substructure for the membrane. The thickness of the dense skin layer can range between 0.1 and 1.0 μm depending on the polymer, composition of the casting solution, speed of casting and immersing, and rate of demixing. The casting speed of large casting machines varies from 1 to 2 m/min for casting solutions with delayed precipitation, such as cellulose acetate, to 10 m/min for fast demixing casting solutions, such as polyethersulfone.

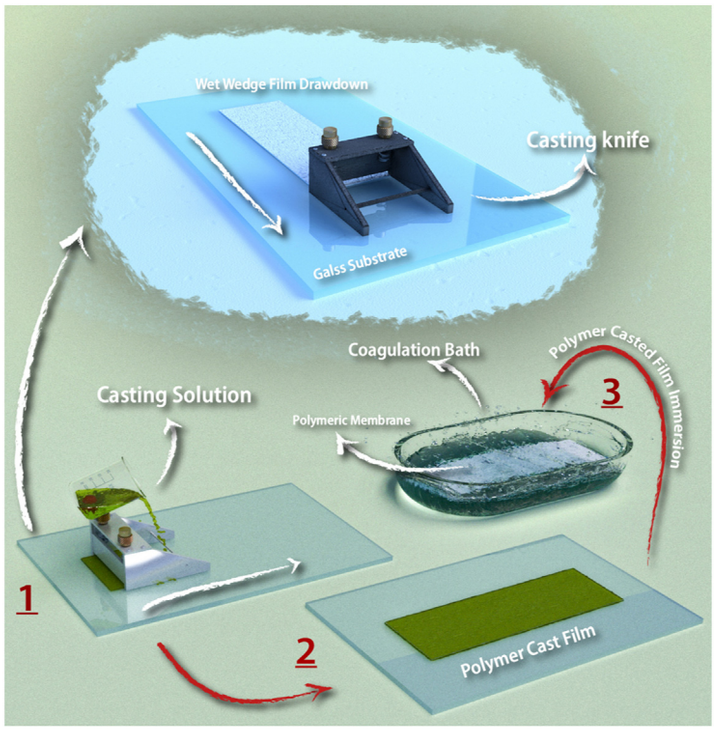

f0010 **FIGURE 1.1** Lab-scale hand-held casting knife, which is typically used to fabricate nonsolvent-induced phase separation (NIPS) membranes. Three main stages include (1) pouring the polymer solution on a suitable support, (2) casting the polymer solution, and (3) placing the cast film in the coagulation bath to initiate solvent-nonsolvent exchange.

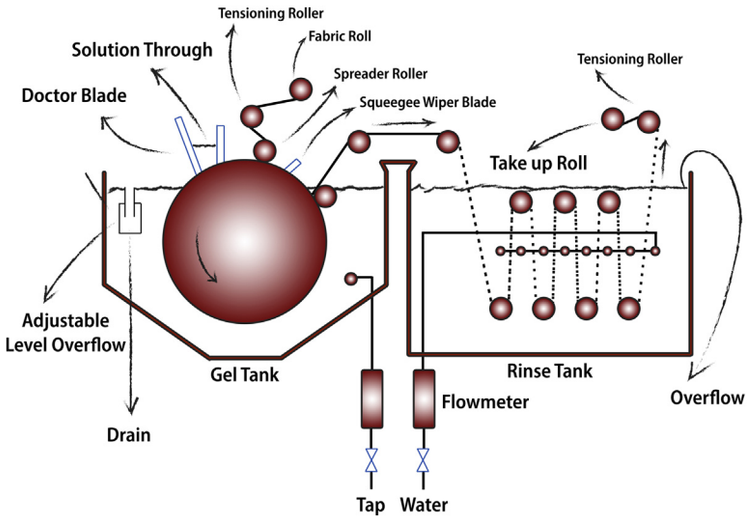

f0015 FIGURE 1.2 Schematic and pilot-scale used to fabricate flat sheet membranes via nonsolvent-induced phase separation (NIPS) [13].

p0030 The preparation procedures for hollow fiber and capillary membranes are quite different since these membranes are self-supported, as shown in Fig. 1.3. In fact, hollow fiber and capillary membranes are not cast on a porous substrate. During the fabrication of hollow fiber membranes, coagulation occurs at both internal and external surfaces. The internal skin morphology can be controlled by controlling the internal coagulation via a proper selection

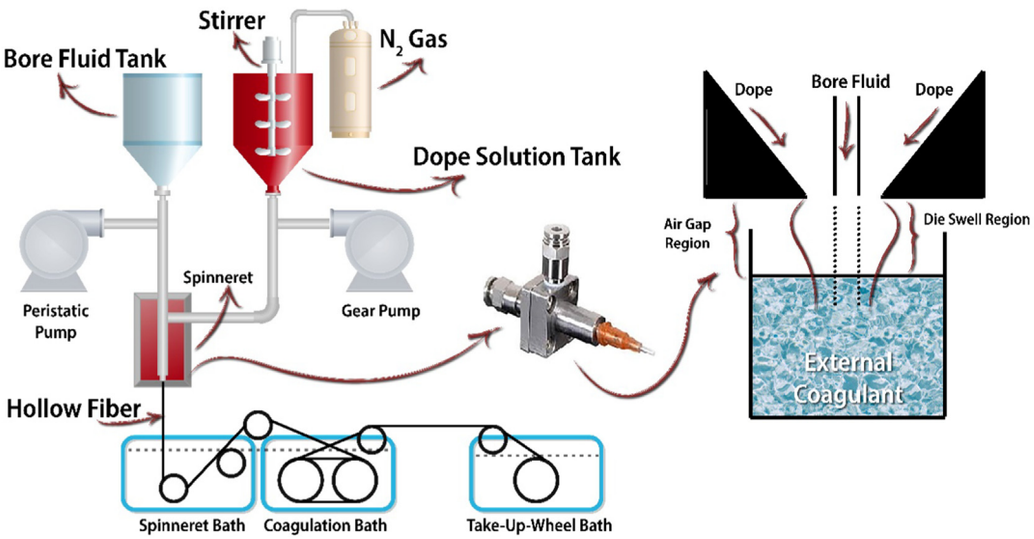

f0020 FIGURE 1.3 Schematic of the spinning system to fabricate hollow fiber membranes.

of the bore fluid chemistry and flow rate. The appropriate choice of the internal coagulant is also crucial because the rate of precipitation and the resultant inner skin layer morphology strongly depend on the chemistry and compositions of the internal coagulant. On the other hand, adjusting the outer coagulant chemistry and coagulation conditions can control the outer skin morphology of hollow fiber membranes. Water is commonly used as an external coagulant to fabricate hollow fiber membranes because of its low cost and environmental friendliness. The surrounding humidity can affect the skin layer morphology in case of a high duration of fiber traveling through the air gap as well as high solvent evaporation at the outer layer of fibers, which induce early precipitation and increase the thickness of the selective skin layer.

p0035 Several key parameters must be considered to fabricate a membrane with desirable mechanical and chemical stabilities and permeation properties. These parameters include the choice of polymer, solvent-nonsolvent system, the concentration of the polymeric mixture, the composition of the nonsolvent bath, and dope casting parameters [29]. To rationalize the impact of these parameters on the structure and properties of resulting membranes, the fundamental principles of the NIPS process need to be understood. The thermodynamic aspect of phase inversion (mainly the phase diagram), the kinetic aspect of solvent and nonsolvent mass transport, and the growth of phase-separated domains (solidification) after phase inversion, are explained in the following section.

s0020 3. Fundamentals and mechanism of NIPS

p0040 Initially, it is essential to understand the phase inversion concept through theoretical principles [30,31]. Although in situ measurements of the phase separation process are difficult, perusing theoretical principles of this process will be helpful to understand NIPS. Generally, membrane formation is based on the thermodynamic and kinetic principles, that is, the relationship between the diffusivities and chemical potentials of the individual components and Gibb's free energy of mixing. A commonly applied method to study the relationship between membrane matrix and its fabrication procedure is to design a ternary polymer/solvent/nonsolvent phase diagram, giving the required information of the thermodynamics and kinetics of the phase inversion process.

s0025 3.1 Thermodynamic principles of NIPS

p0045 The thermodynamic behavior of the NIPS process can be described using a ternary polymer/solvent/nonsolvent phase diagram. Fig. 1.4 shows a classic phase diagram. The angles of the triangle signify the three ingredients (polymer, solvent, and nonsolvent), whereas all possible points within the shape denote a mixture of three parts. The ternary diagram is a simple picture of an actual phase inversion process where more than three components can usually exist in the dope solution and nonsolvent bath.

p0050 The triangle comprises two sections: a single-phase area where all components are soluble and a double-phase area where the mixture splits into polymer-rich and polymer-poor phases. The lines that link a couple of equilibrium compositions within the triangle and the liquid−liquid phase frontier are named a tie line and binodal, respectively. The primary

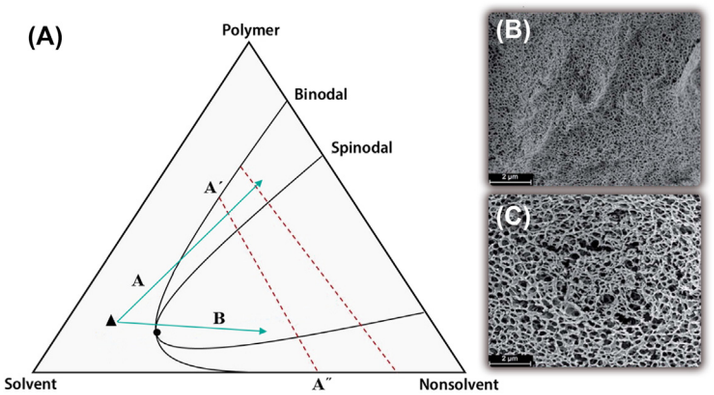

f0025 FIGURE 1.4 (A) A typical ternary phase diagram showing the membrane formation mechanism via nonsolvent-induced phase separation (NIPS) method, and the formation of (B) tighter and (C) more porous structures based on different pathways of solvent-nonsolvent demixing.

polymer dope solution for membrane fabrication is situated on the polymer/solvent axis. Nevertheless, it is also possible to add nonsolvents to the dope solution so that all three parts are still miscible. This single-phase region is located between the polymer/solvent axis, the solvent/nonsolvent axis, and the binodal. By adding nonsolvents to polymer/solvent mixture, the composition of the dope solution moves to the right side of the triangle (pathways A and B). Consequently, demixing will take place when the mixture becomes thermodynamically unstable. As displayed in Fig. 1.4, the point where binodal and spinodal curves intersect, the so-called critical point, is located at low or very low polymer contents.

p0055 There are two potential pathways for the dope solution to solidify: pathway A, which leads to binodal demixing, and pathway B, which leads to spinodal decomposition. In pathway A, the dope solution finishes up at the metastable area, between the binodal and spinodal curves, where the polymer solution is thermodynamically unstable, but the polymer precipitation does not happen. Here, the dope solution is possibly converted to a polymer-rich phase (point A′) and a polymer-poor phase (point A″) based on the nucleation and growth mechanism. These compositions within the triangle (A′ and A″) are connected by means of tie lines. Two points at each side of tie lines are at thermodynamic equilibrium.

p0060 When the dope solution passes across the binodal and spinodal border without having adequate time to initiate the demixing process, spinodal decomposition happens (pathway B). In this situation, the polymer solution directly finishes up in the thermodynamically unstable area within the spinodal region. Similar to the binodal region, two phases will emerge when the dope solution moves in pathway B; however, it is expected to have two cocontinuous phases that will finally lead to nuclei formation instead [32,33]. The polymer concentration and hence pathway above the critical point can usually represent the fabrication of a solidified membrane.

p0065 As shown in Fig. 1.5, there are four regions in the ternary phase diagram of polymer/solvent/nonsolvent: (I) a homogenous solution phase, (II) liquid−liquid phases, (III) liquid−solid phases, and (IV) solid phase. Basically, if the system starts from point *A* in region I, the system can follow four different pathways [34]. If the system reaches point S_1 in the diagram, liquid−liquid phase inversion occurs, resulting in phase S_2 (polymer-rich phase) and phase S_3 (polymer-lean phase). When S_1 is located in the metastable region between binodal

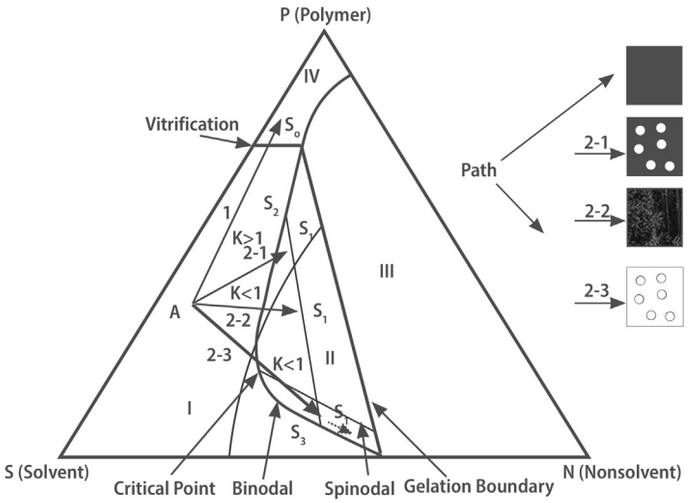

FIGURE 1.5 Ternary phase diagram describing different pathways, in more detail, of membrane fabrication via nonsolvent-induced phase separation (NIPS) process [34]. f0030

and spinodal curves at high polymer concentration, membrane formation takes place through nucleation and growth mechanism of the polymer-lean phase, resulting in noninterconnected pores.

p0070 On the other hand, a bicontinuous structure with interconnected pores can be formed through path 2-2, in which the system enters directly into the unstable region where solidification carries out. When the system follows path 2-3, it enters a metastable region at low polymer concentration, producing membranes with low integrity. Two further definitions related to the thermodynamics of phase inversion are (i) delay time and (ii) gelation time. The time interval between the immersion in the nonsolvent and the start of the liquid–liquid demixing is defined as delay time. From the phase diagram, it can be found that the system can cross different regions based on the delay time, leading to the formation of a membrane with different morphology. For fast or instantaneous demixing, the system immediately enters the unstable region, while in case of delayed demixing, the system stays in the metastable region before it reaches the unstable region. The gelation time is usually considered as the time interval between the onset of the demixing and the solidification of the polymer solution.

p0075 The formation of the final membrane structure is a complicated process in which all the mechanisms described above can be involved. Nucleation and growth, solidification, and gelation significantly influence the final structure of the membrane. When phase inversion proceeds through nucleation and growth, the formation of interconnected pores will be promoted by increasing the gelation time.

s0030 3.2 Kinetic principles of NIPS

p0080 The kinetics of phase inversion induced by nonsolvent is mainly affected by the solvent/nonsolvent exchange rate in the coagulation bath. In fact, the mass transfer during solvent/

nonsolvent exchange defines the path on the membrane phase diagram. The chemical potential gradient between the solvent and nonsolvent is known as the driving force for each component. To characterize the kinetics of NIPS process, the penetration of nonsolvent into the cast film needs to be investigated [35–37]. Upon the first contact with the nonsolvent bath, the chemical potential gradient is the greatest near the borderline between the polymer solution and the nonsolvent, presenting the quickest exchange rate. Nevertheless, the solvent/nonsolvent exchange rate will decrease over time due to the reduction of chemical potential gradient, as presented in Fig. 1.6. At this time, an asymmetric membrane with a lower permeable surface layer that controls mass transfer rate will be fabricated. On the other hand, several factors influence the exchange rate, such as the size of the molecules penetrating in or out, as well as the viscosity of the media that the particles transport through [38,39]. Possible morphologies of membranes generated from the NIPS process could be ascribed to the thermodynamics and kinetics of phase separation. The formation of macrovoids is also attributed to the kinetic hindrance and the hydrodynamic instability induced by gradient at the interface [35], precipitation rate [36], and the surplus intermolecular gradient driven by interfacial concentration gradient [40].

p0085 As mentioned earlier, once the cast film is being exposed to the nonsolvent, liquid-liquid separation occurs in which two possible types of demixing, delayed and fast demixing, rely upon the solvent/nonsolvent exchange rate. These two types of demixing result in two pathways of membrane formation on the phase diagram, leading to the formation of various structures, as shown in Fig. 1.7. After the first contact between the cast film and the nonsolvent, if the membrane wall is shaped very fast, the immediate demixing occurs; otherwise, if there is an adequately long time for the formation of membrane pores, the delayed demixing occurs [13,41,42].

p0090 It is to be noted that there are no principles to put time boundaries between the immediate and delayed demixing processes. A membrane with an approximately uniform porous top layer is formed as a result of immediate demixing (Fig. 1.7B). In this type of membrane,

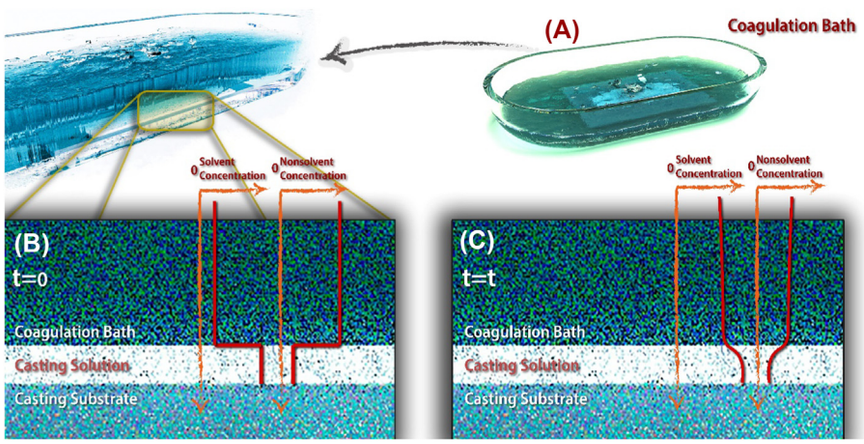

f0035 FIGURE 1.6 Concentration profiles of solvent and nonsolvent during NIPS process, right after plunging in the nonsolvent (A), at the initial time (B) and after a time t (C) for a polymer solution containing some nonsolvent [38].

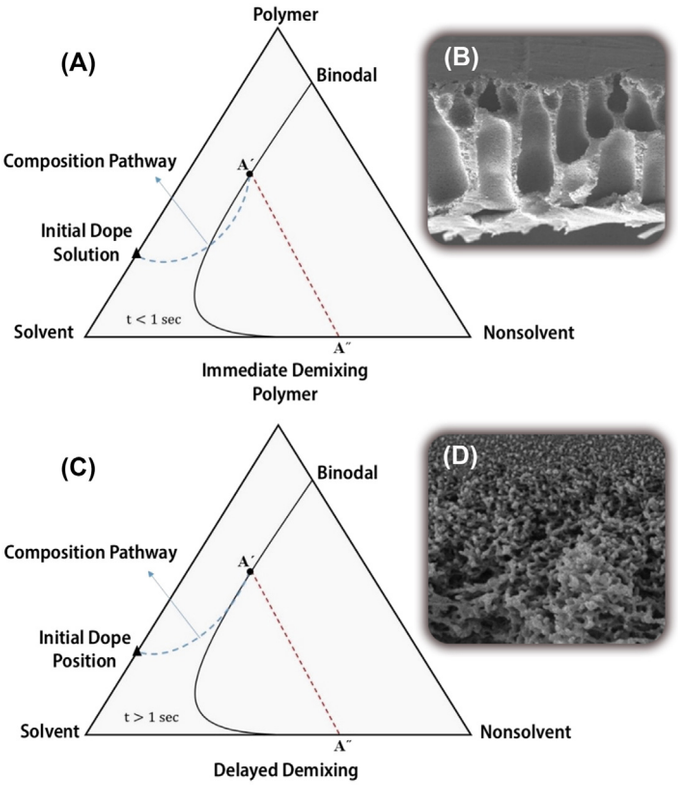

FIGURE 1.7 Schematic phase diagram of immediate (A and B) and delayed (C and D) demixing process. f0040

finger-like pores (or macrovoids) can be observed in the support layer (Fig. 1.8A). The membranes formed with delayed demixing would possess an approximately denser top layer (Fig. 1.7D), resulting in lower permeability than the membranes formed due to immediate demixing (Fig. 1.8B). The morphology of membranes produced via the NIPS process results from the interplay between thermodynamic and kinetic parameters during phase inversion. For example, the formation of unwanted finger-like macrovoids can be hindered by using a weak nonsolvent, a mixture of water and glycerol or water and n-methyl-2-pyrrolidone (NMP). The addition of solvent in the coagulation media slows the solvent–nonsolvent exchange rate and thus delays the nonsolvent influx, which is responsible for voids growth. The influence of glycerol is connected to its lower nonsolvent power as well as its viscosity, which further delays the nonsolvent influx. However, it must be noted that important variables like polymer concentration, solvent/nonsolvent miscibility degree, and coagulation bath composition have the most impact on the precipitation process.

p0095 The final membrane structure and morphology also depend on the polymer type being used for membrane fabrication. For glassy polymers, such as polysulfone (PS), cellulose acetate (CA), and polyimide (PI), phase inversion is mainly controlled by liquid–liquid demixing, whereas, for semicrystalline polymers, such as polyvinylidene fluoride (PVDF),

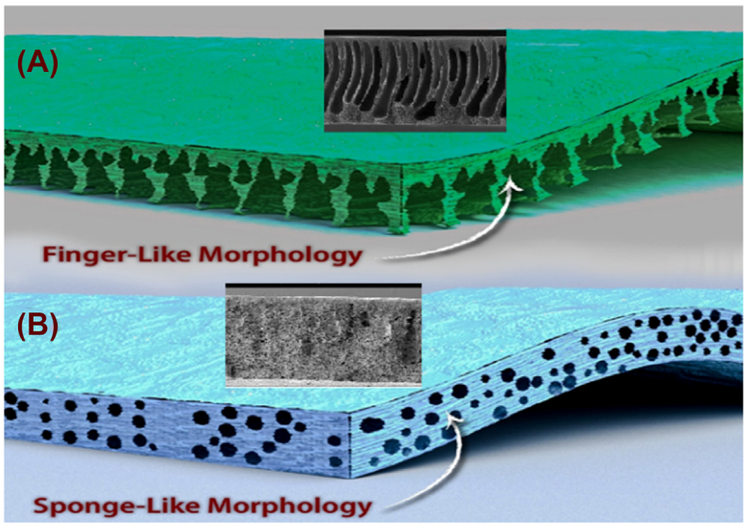

f0045 FIGURE 1.8 Various membrane structures formed by different types of demixing: (A) Immediate demixing and (B) delayed demixing.

solid–liquid demixing and polymer crystallization may also occur during phase inversion. Usually, liquid–liquid demixing leads to the formation of membranes with cellular morphology and/or finger-like macrovoids. In contrast, phase inversion facing solid–liquid demixing often results in a particulate structure made of interlinked semicrystalline spherulites.

s0035 ### 3.2.1 *Kinetic model of mass transfer in the NIPS process*

p0100 A reliable kinetic model can be developed by solving the problem of moving boundary transport in which the following aspects should be accounted for, as adopted by Ahmad et al. [43].

o0010 **(i)** nonsolvent non-quasi-stationary diffusion across the solidified membrane
o0015 **(ii)** changing the nonsolvent concentration in the coagulation bath
o0020 **(iii)** membrane swelling with the time during the NIPS process

p0120 Some assumptions should be made to describe the kinetics of the NIPS process for the problem of moving boundary transport as below.

o0025 **(i)** The dope solution is a completely homogeneous solution and the surface area of cast film is constant during the NIPS process. It is also considered that the swelling/shrinkage takes place in just z-direction.
o0030 **(ii)** Liquid–liquid demixing occurs while phase separation is very fast and the kinetics of this process is controlled by counter-diffusion of nonsolvent in coagulation bath and solvent in casting solution through the membrane porous substrate.
o0035 **(iii)** The amount of solvent and nonsolvent exchanged are equal.

o0040 **(iv)** During measuring the density of dry porous membranes, the density of air is assumed to be neglected.

o0045 **(v)** The deviation from the isothermal behavior of the casting solution and coagulation bath is also neglected.

p0150 According to these assumptions and Fig. 1.9, the nonsolvent concentration profile in the membrane film during the phase separation process can be theoretically formulated under "unsteady state" condition as follows:

$$D\frac{\partial^2\overline{C}}{\partial z^2}=\frac{\partial\overline{C}}{\partial t};(Z_c\le z\le H;t>0 \tag{1.1}$$

where D is nonsolvent molecular diffusion coefficient through the solid film (membrane), $\overline{C}$ is nonsolvent mass concentration (time-dependent) in the membrane film, Z is z-direction in cartesian coordinate, $Z_c(t)$ is axial position of the moving solidification (time-variant), which can be measured from the membrane casting plate. The initial and boundary conditions for the above equation are:

$$C=C_0;(t=0) \tag{1.2}$$

$$\overline{C}=\lambda C\ ;\ (z=H,t>0 \tag{1.3}$$

$$\overline{C}=0;(z=Z_C) \tag{1.4}$$

$$D\frac{d\overline{C}}{dz}=\frac{1}{A}\frac{dM_{ns}}{dt};(z=Z_c,\ t>0) \tag{1.5}$$

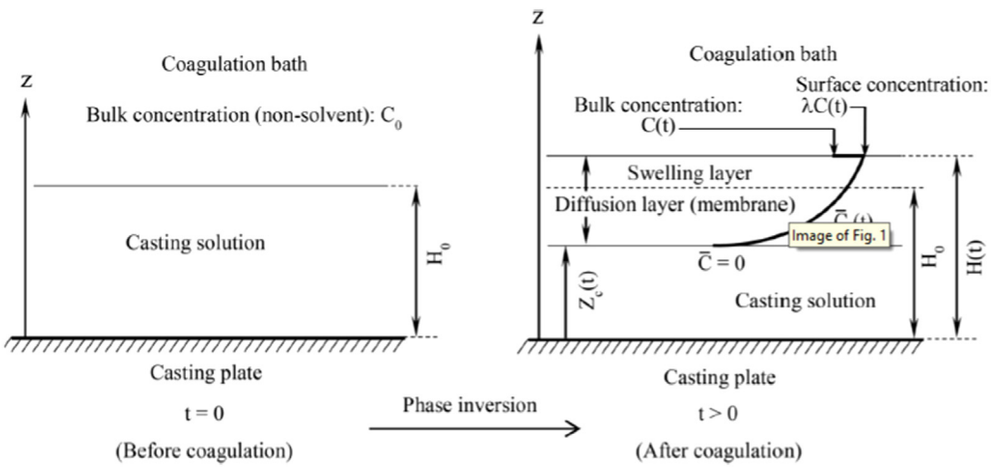

f0050 **FIGURE 1.9** Theoretical concentration profile of nonsolvent in the solidified membrane [43].

where C_0 and $C(t)$ are the initial and time-dependent mass concentration of nonsolvent (water) in the coagulation bath, respectively, λ is the mass distribution coefficient of nonsolvent at the membrane surface, $H(t)$ and A are the membrane thickness and surface area, and M_{ns} is nonsolvent mass through the diffusion layer. The left- and right-hand sides of Eq. (1.5) represent the nonsolvent diffusive mass flux in the solidification zone and influx caused by liquid–liquid demixing, respectively. The following mass balance equation can be applied for the exchange of nonsolvent and solvent during the phase inversion process at a given moving boundary transport problem:

$$V_{cb}C_0 = V_{cb}C(t) + \int_{Z_c}^{H} A\overline{C}nsdz \tag{1.6}$$

where V_{cb} is the volume of coagulation bath, $\overline{C}_{ns}$ is nonsolvent capacity in the membrane solidified. The initial amount of nonsolvent in the coagulation bath was represented on the left-hand side of this equation. The first term on the right-hand side describes the nonsolvent variation, and the second term denotes the nonsolvent amount utilized for the solidification. After simplification, Eq. (1.6) can be rewritten as:

$$C = C_0\left[1 - \propto \left(H^* - Z_c^*\right)\right] \tag{1.7}$$

where

$$\propto = \frac{AH_0\overline{C}ns}{C_0V_{cb}}, H^* = \frac{H}{H_0}, Z_c^* = \frac{Z_c}{H_0} \tag{1.8}$$

α represents the nonsolvent mass fraction in the diffusion area, H_0 describes the initial thickness of cast film before precipitation. Under the assumption of fully insoluble polymer in nonsolvent, the mass of casting solution that undergoes solidification at any time can be obtained by:

$$M_{cs} = \rho_{cs}A(H_0 - Z_C) \tag{1.9}$$

Where ρ_{cs} is the mass density of casting solution and membrane. Similarly, the quantity of casting solution solidifies over time can be calculated by:

$$M_{memb} = \rho_{memb}A(H - Z_c) \tag{1.10}$$

Where ρ_{memb} is the mass density of the membrane. By balancing polymer in casting solution and membrane at any time, the following equation is obtained:

$$\rho_{cs}A(H_0 - Z_C)f_{poly} = \rho_{mem}A(H - Z_c) \tag{1.11}$$

Where f_{poly} is the mass fraction of polymer in the casting solution. The membrane swelling during solidification can be obtained with the following equation, which is a simplification of Eqs. (1.8) and (1.11):

$$H^* = k + (1-k)Z_c^* \tag{1.12}$$

where $k = \rho_{cs}.f_{poly}/\rho_{memb}$, which is called membrane swelling/shrinkage factor. For $k > 1$, the liquid–liquid demixing results in swelling of the membrane, while for the $k < 1$, the membrane shrinks. There will be no shrinkage and swelling when $k = 1$. The k parameter can also be estimated accurately by measuring the slope and intercept of the H^* versus Z^*_c plot obtained from Eq. (1.12). The following mass balance can be used at any time of phase inversion in which "b" is a required mole of nonsolvent per mole of solvent during solidification of casting solution or formation of membrane:

$$\frac{1}{b}\frac{dM_{ns}}{dt} = \frac{dM_{cs}}{dt} \tag{1.13}$$

p0155 Therefore, the boundary conditions in Eq. (1.5) reduce to the following equation by using Eqs. (1.9) and (1.13):

$$D\frac{d\overline{C}}{dz} = -bH_0\rho_{cs}\frac{dZ_c^*}{dt} \tag{1.14}$$

p0160 By combining Eqs. (1.7) and (1.12), Finally, the bulk concentrations of nonsolvent, which vary with time, are determined from the following equation:

$$C^* = 1 - \propto k\left(1 - Z_c^*\right) \tag{1.15}$$

Where: $C^* = \dfrac{C}{C_0}$

s0040 3.3 Solubility parameters

p0165 In the phase inversion process, the solubility parameters of casting solution components are of great importance. They are usually employed to evaluate the possible interactions between the polymer–solvent, solvent–nonsolvent, and polymer–nonsolvent. These interactions describe the ability of the solvent to dissolve a polymer, the miscibility of solvent–nonsolvent, and the nonsolvent power toward a polymer, respectively. Therefore, the final morphology of the membrane will be strongly affected by these mutual interactions through changing the thermodynamic enhancement and kinetic hindrance of phase inversion. In general, two compatible chemical species have closer solubility parameters. For instance, with a slight difference between the solubility parameters of polymer and solvent, the dissolving capacity of solvent is high, and as a consequence, the rate of liquid–liquid demixing is decreased. If the difference between the solubility parameters of polymer and nonsolvent parameters is high, nonsolvent has a strong power to precipitate the polymer, and as a consequence, fast liquid–liquid demixing takes place. The difference between the solubility parameter of nonsolvent and solvent strongly influences their exchange rate during phase inversion.

p0170 For a pure liquid substance, the square root of the cohesive energy density is used to obtain the Hildebrand solubility parameter, δ, as below:

$$\delta = \sqrt{\left(\frac{\Delta H_{\mathrm{v}} - RT}{V_{\mathrm{m}}}\right)} \tag{1.16}$$

Where ΔH_{v} is the heat of vaporization and V_{m} is the molar volume.

p0175 According to Hansen's theory [44], δ can be calculated using the energy from dispersion bonds (δ_d), the energy from hydrogen bonds between molecules (δ_h), and the energy from dipolar intermolecular forces (δ_p) as below:

$$\sqrt{\left(\delta_d^2 + \delta_p^2 + \delta_h^2\right)} \tag{1.17}$$

p0180 The method of calculating δ_d and δ_p is presented by Blanks and Prausnitz [45]. Calculation of δ_p is described by Hansen and Beerbower as follows:

$$\delta_p = 37.4\frac{\mu}{\mathrm{V}^{0.5}} \tag{1.18}$$

where V is the solvent molar volume and μ is the solvent dipole moment. The group contribution technique is the best one for computing δ_h. A new variable, R_a, was developed by Skaarup [44] as solubility parameter distance of polymer (ingredient 1) and solvent (ingredient 2) and their affinity to each other, which is equal to:

$$R_a = \sqrt{4(\delta_{d2} - \delta_{d1})^2 + (\delta_{p2} - \delta_{p1})^2 + (\delta_{h2} - \delta_{h1})^2} \tag{1.19}$$

p0185 Therefore, the interactions between pair of polymer–solvent (P–S), polymer–solvent (P–NS), and solvent–nonsolvent (S–NS) can be calculated by the following equations [46]:

$$\mathrm{P-S}\colon \delta_{\mathrm{P,S}} = \sqrt{(\delta_{d,P} - \delta_{d,S})^2 + (\delta_{p,P} - \delta_{p,S})^2 + (\delta_{h,P} - \delta_{h,S})^2} \tag{1.20}$$

$$\mathrm{P-NS}\colon \Delta\delta_{\mathrm{P-NS}} = \sqrt{(\delta_{d,P} - \delta_{d,NS})^2 + (\delta_{p,P} - \delta_{p,NS})^2 + (\delta_{h,P} - \delta_{h,NS})^2} \tag{1.21}$$

$$\mathrm{S-NS}\colon \Delta\delta_{\mathrm{S-NS}} = \sqrt{(\delta_{d,S} - \delta_{d,NS})^2 + (\delta_{p,S} - \delta_{p,NS})^2 + (\delta_{h,S} - \delta_{h,NS})^2} \tag{1.22}$$

p0190 The top-surface morphology of membrane is more related to the affinity or solubility parameter between polymer and nonsolvent, whereas the exchange rate of solvent–nonsolvent was found to more affect the sublayer pore structure. As discussed earlier, a lower affinity between polymer and solvent will increase the phase inversion rate, resulting in a porous top layer. However, if the solvent has a lower diffusion rate in the coagulation bath, delayed solidification takes place, leading to developing macrovoids in the sublayer. This can also increase the overall thickness of the membrane. The use of solvent mixtures in the casting solution could delay the solvent–nonsolvent exchange, promoting the macrovoid growth in the sublayer.

s0045 3.4 Mechanism of macrovoid formation

p0195 The sponge structure versus the finger-like structure of the membrane fabricated through NIPS is an obvious example of a trade-off between thermodynamic and kinetic parameters. The formation of macrovoids represents an unwanted morphology which leads to lower the mechanical strength of the membrane. Different mechanisms are proposed to explain the macrovoids formation. Instabilities of interfacial hydrodynamic, driven by surface tension gradients, can be a possible mechanism for macrovoid initiation. Ray et al. [47] and Smolders et al. [48] connected the macrovoids formation to the concentration gradients at the casting solution and the nonsolvent interface and to the type of demixing, that is, instantaneous or delayed, respectively. They proposed that macrovoids are generated under the skin layer of the membrane if the solvent concentration increases to a certain threshold value and if the composition of the solution in front of the nuclei remains stable for a suitable period. The most well-known and widely accepted mechanism for macrovoid formation is instantaneous demixing of dope solutions during precipitation which was proposed by Smolders et al. [20]. This type of demixing will result in the nucleation of the polymer-lean phase that absorbs the solvent surrounding them and then grows into macrovoids. It was pointed out that the driving force for the nucleation and growth is the solvent concentration difference in the polymer-lean phase and the casting solution surrounding them. A continuous polymer-lean phase is generated if the phase inversion mechanism is based on spinodal decomposition, not nucleation and growth. Hence, there are no nuclei that can grow into macrovoids. For membranes fabricated via nucleation and growth mechanism, the macrovoids are mainly generated right beneath the membrane surface (Fig. 1.10A), indicating that macrovoids initiate at a high mass transport rate of solvent and nonsolvent. On the other hand, for membranes prepared via spinodal decomposition, macrovoids generate at deeper positions near to bottom layer (Fig. 1.10B), indicating that the fastest mass transport position is not the position to initiate the macrovoids. The formation of macrovoids can be avoided by delayed demixing by increasing the polymer and/or nonsolvent concentration in the casting solution. Some other methods to decrease the macrovoids formation are the addition of

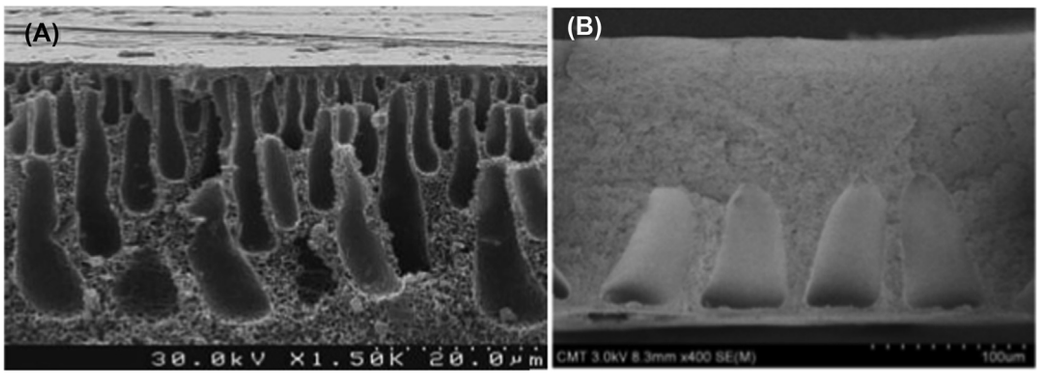

f0055 FIGURE 1.10 Cross-sectional SEM images of PSf membranes prepared by NIPS process: (A) macrovoids right beneath the membrane surface; (B) macrovoids at the bottom of membrane structure [50].

solvent into the nonsolvent bath [49], and the addition of organic additives such as polyvinylpyrrolidone (PVP) in the casting solution [50], and the evaporation of solvent from cast film [51].

s0050 3.5 Influential parameters on membrane morphology in the NIPS process

p0200 The key factors that affect membrane formation via the NIPS method are discussed in the following sections. These factors include the type of polymer, composition of the dope solution, the solvent-nonsolvent system, the coagulation bath composition, and casting conditions [28,40,52–57].

s0055 *3.5.1 Choice of solvent/nonsolvent system*

p0205 Solvent/nonsolvent system in the NIPS process substantially affects the membrane structure, mechanical characteristics, interfacial properties, and separation performance. The solvent must easily dissolve the polymer at a concentration up to 25 weight percent and must also have high miscibility with nonsolvent in the coagulation bath. Table 1.1 represents suitable solvents for cellulose acetate (CA), polysulfone (PSf), polyvinylidene fluoride (PVDF), and polyacrylonitrile (PAN) [58–61]. The aprotic solvents such as NMP, DMF, and DMAc can easily dissolve many polymers such as PES, PSf, PVDF, and PAN. The prepared dope solutions precipitate rapidly when immersed in nonsolvent (water). The resultant membranes usually have an asymmetric and porous structure because of the high affinity of these solvents and water as nonsolvents. However, these aprotic solvents are toxic and potentially hazardous to the environment and health. Therefore, an important issue in selecting the suitable solvent for membrane fabrication is to use green or nontoxic solvents to protect the environment and human health.

p0210 Numerous solvent/nonsolvent pairs possess their own particular thermodynamic properties and solubility. Usually, when a solvent/nonsolvent pair shows higher affinity to each other, the immediate demixing will be more likely, leading to the formation of a porous

t0010 **TABLE 1.1** Possible solvents for four common polymers.

	Polymer			
Solvent	**CA**	**PSf**	**PVDF**	**PAN**
	Dimethylformamide (DMF)	Dimethylformamide (DMF)	Dimethylformamide (DMF)	Dimethyl sulfone (DMSO2)
	Dimethylacetamide (DMAc)	Dimethylacetamide (DMAc)	Dimethylacetamide (DMAc)	Dimethylsulfoxide (DMSO)
	Acetone	N-Methylpyrrolidone (NMP)	N-Methylpyrrolidone (NMP)	Ethylene carbonate (EC)
	Tetrahydrofuran (THF)	Dimethylsulfoxide (DMSO)	Dimethylsulfoxide (DMSO)	Propylene carbonate (PC)
	Dimethylsulfoxide (DMSO)	Morpholine (MP)	Tetramethylurea (TMU)	Dimethylformamide (DMF)

structure [13]. In contrast, when the solvent/nonsolvent pair shows lower affinity, the delayed separation occurs during the NIPS process, and as a result, an asymmetric membrane with a dense surface layer will be formed.

p0215 Flory and Huggins have introduced a two-dimensional lattice model to calculate polymer solubility [62–64]. An assumption is considered in this model where the solvent molecules and polymer sector are of a similar size and also just one of them can settle in a lattice side. The Gibbs free energy (ΔG_m) of the solution is computed by:

$$\Delta G_m = kT(n_1 \ln \varphi_1 + n_2 \ln \varphi_2 + \chi_{12} n_1 \varphi_2) \tag{1.23}$$

Here, φ is the volume fraction, n_1 and n_2 are the molecule number of solvent (1) and polymer (2), T is the absolute temperature, k is the constant number of Boltzmann, and χ_{12} is the Flory interaction parameter that demonstrates the interaction energy of polymer–solvent mixture. χ_{12} is calculated commonly by the experimental approach of reverse gas chromatography [65]. Flory-Huggins model was modified to explain polymeric dilute solutions [66] and to evaluate χ_{12} (dependent on concentration) [67].

p0220 A newly defined variable, δ, is utilized to determine χ_{12}, which helps to choose a desirable solvent-polymer combination. The solubility of solvents is calculated as

$$\delta = \sqrt{\frac{\Delta E^{\nu}}{V}} \tag{1.24}$$

where ν is molar volume, and ΔE^{ν} is the vapourization molar energy, which is attributed to the enthalpy as $\Delta E^{\nu} \approx \Delta H^{\nu} - RT$ [68]. The Flory interaction parameter is calculated by means of the following equation:

$$\chi_{12} = \frac{\nu_1}{RT}(\delta_1 - \delta_2)^2 \tag{1.25}$$

where R is the ideal gas constant, ν_1 is the molar volume, δ_1 is the solubility parameters of solvent, and δ_2 is the solubility of polymers, which is approximated experimentally by dissolving polymers in various solvents. Furthermore, the heat of mixing (ΔH_m) has been described by Scatchard and Hildebrand as:

$$\Delta H_m = V_m(\delta_1 - \delta_2)^2 \varphi_1 \varphi_2 \tag{1.26}$$

Here, V_m is the molar volume. Eq. (1.26) is limited to just $\Delta H_m > 0$ and not applicable for specific interactions.

s0060 ### 3.5.2 *Choice of polymer*

p0225 The separation performance of porous membranes is mainly determined by the pore size distribution. This parameter is more strongly affected by the methods and conditions used for membrane fabrication than by the properties of the utilized polymer. But, the intrinsic properties of the polymer directly affect the chemical and thermal stability, surface hydrophilicity, and solute adsorption of the resultant membrane. The choice of an appropriate polymer is more important in a dense membrane than in a porous membrane due to its direct influence

on the solubility and diffusivity of the membrane. Nevertheless, in the NIPS process, the choice of polymer is crucial because it limits the choice of solvent/nonsolvent pair. Various polymers are currently used to fabricate MF, UF, and NF membranes, including PSf, PES, PVDF, PAN, and CA [69–71]. Water is the most available and cheapest nonsolvent that can be used in the NIPS process and shows good affinity with a large number of polar solvents [21,72–75]. Generally, the choice of a suitable polymer depends on the membrane application. For example, the applied membranes in the MD process must be hydrophobic [20,76–78]. Hence, a group of fluoropolymers like PVDF and polytetrafluorethylene (PTFE) are good choices [79–81]. On the other hand, for water treatment applications where "water-removing" membranes are needed, hydrophilic polymers such as PAN, PES, and PAI are excellent candidates [2,16,82–84].

s0065 ### 3.5.3 *Polymer concentration*

p0230 The polymer concentration in the casting solution is another crucial parameter that influences the membrane morphology fabricated by the NIPS method. Usually, polymer concentration varies from 10 to 30 wt%, in which a concentration lower than 20 wt% is used to fabricate the porous membranes [85]. Increasing the polymer concentration enhances dope solution viscosity and the polymer content in the casting solution, resulting in kinetic hindrance and the formation of denser structures [86]. The increase in polymer concentration of casting solution leads to a decrease in the mass transport of nonsolvent, which makes the composition stay longer in the metastable region (Fig. 1.11), and also makes the casting solution easier to gel and get more stable because of higher viscosity. Therefore, the polymer concentration effect on the phase inversion mechanism depends on the competition between its impact on mass transport rate and stability. If the increase in mass transport dominates, nucleation and growth mechanism occur, and the cellular structure forms. On the other hand, if the increase in stability dominates the phase inversion mechanism, solidification takes place and bi-continuous structure forms, creating pores with high connectivity.

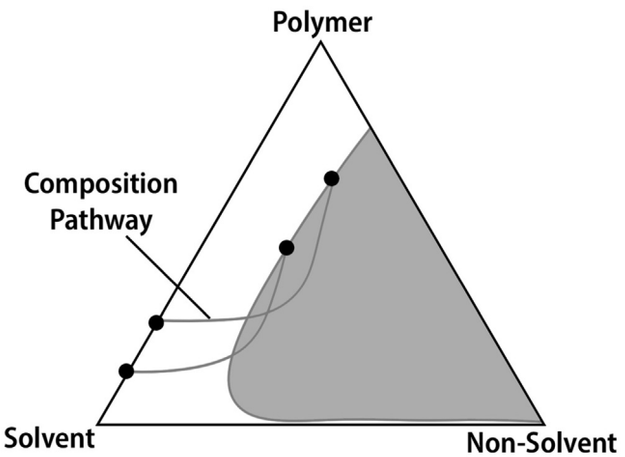

f0060 FIGURE 1.11 Schematic of composition pathways for different concentrations of polymer in the casting solution. Pathway (A) low polymer concentration and pathway and (B) high polymer concentration.

s0070 ***3.5.4 Composition of the coagulation bath***

p0235 Choosing the proper nonsolvent will strongly affect the rate of precipitation of cast film during the NIPS process. The solvent/nonsolvent miscibility degree and the affinity between nonsolvent and polymer greatly influence the phase inversion and the membrane morphology. As mentioned earlier, water is the most frequently used nonsolvent, while other nonsolvents like acetone and lower aliphatic alcohols can also be applied [87–89]. Sometimes, a certain amount of solvent is added to the coagulation bath to control and optimize the NIPS process [21]. Nevertheless, the binodal border limits the amount of solvent added to the bath. When a solvent is added to the coagulation bath, the membrane formation pathway shifts from the immediate demixing to the delayed one, as shown in Fig. 1.12B. In other words, the addition of extra solvent to the polymer/solvent/nonsolvent system decreases the

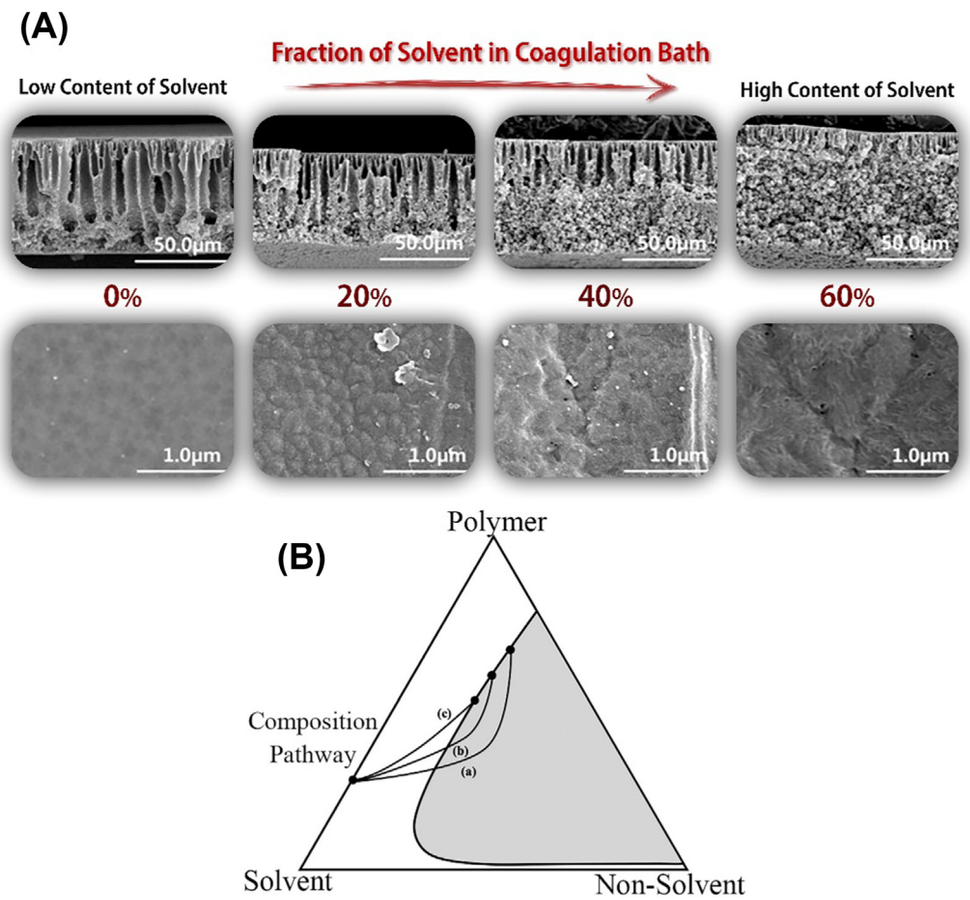

f0065 **FIGURE 1.12** The effect of solvent content in the coagulation bath on (A) membrane morphology and (B) ternary phase diagram showing demixing shifts from instantaneous to delayed with increasing solvent concentration (from pathways a to c) [90].

polymer concentration at the film interface and nonsolvent diffusion rate into the film, which eventually delays the separation process and leads to the formation of a denser structure for membrane (Fig. 1.12A) [21]. In addition to the solvent, adding other additives such as methanol, surfactants, and salt into the nonsolvent bath was found to affect the membrane formation [91–94].

s0075 ### 3.5.5 Composition of the casting solution

p0240 The nonsolvent can be added to the casting solution as an efficient modifier to tailor the morphology and separation performance of membranes. As shown in Fig. 1.13, adding an appropriate amount of nonsolvent in the polymer solution causes the composition path to cross the binodal curve faster, resulting in instantaneous demixing during phase inversion. The induced instantaneous demixing by adding nonsolvent in the casting solution can be due to increasing the thermodynamic instability of the casting solution by adding nonsolvent, which can promote the macrovoid formation [90]. However, for a casting solution subjected to instantaneous demixing, adding nonsolvent in the casting solution suppresses macrovoid formation and growth because the nonsolvent in the casting solution accelerates the phase separation considerably. The nonsolvent addition in the casting solution is practically used to make the membrane with high porosity. The mass transport during immersion precipitation increases the polymer concentration at the cast film-nonsolvent interface because of the higher solvent outflux compared to the nonsolvent influx. An increase in the thermodynamic instability of the casting solution results in a decline in polymer concentration at the interface. Hence, the membranes with a higher surface porosity are usually fabricated by adding a large amount of nonsolvent in the casting solution.

s0080 ### 3.5.6 Additives to the dope solution

p0245 In practice, the composition of casting solutions varies based on the customer demand and type of separation application. It often contains different kinds of additives (usually 5–20wt%) to obtain desired membrane morphology and separation performance. Additives are used to hinder the formation of macrovoid, improve pore formation and their

f0070 FIGURE 1.13 Schematic representation of the composition paths for different nonsolvent concentrations in the casting solution.

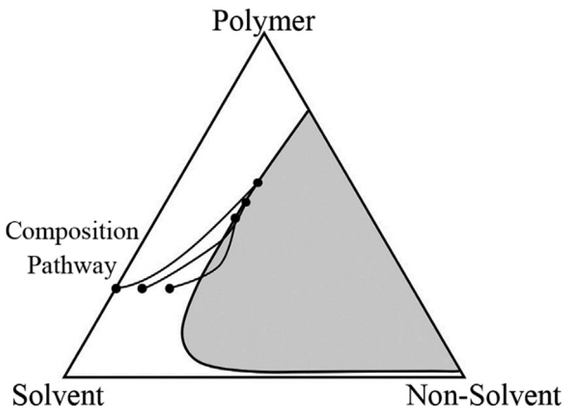

connectivity, and enhance the membrane hydrophilicity. The presence of additives in the casting solution makes membrane fabrication much more complicated since it becomes impractical to conduct comprehensive theoretical analyses on the thermodynamic and kinetic mechanism of the phase inversion process. Various types of materials like cosolvents [95,96], nonsolvent [96,97], particles, or polymeric additives can be added to the dope solution to obtain a desirable membrane [40,98–102]. These additives (organic or inorganic) can either form a dispersed phase [103–107] or can be fully dissolved. Nonsolvent activity, viscidity, volatility, and contents of added materials are the definite attributes influencing the final membrane structure and performance [108–113].

p0250 The common additives used to prepare polymer solutions are generally water-miscible, which are nonsolvent to the main polymers [114–116]. These additives enhance the thermodynamic instability of the casting solution, increasing the nonsolvent influx to the cast polymer film. This effect accelerates the phase inversion process, leading to the fabrication of a more porous structure (called the thermodynamic enhancement). At the same time, the presence of additives increases the viscosity of the casting solution, which decreases the solvent–nonsolvent exchange rate, leading to a delayed phase inversion and the formation of a less porous structure (called kinetic hindrance). Therefore, the combination of thermodynamic enhancement and kinetic hindrance would play an essential role in understanding the impact of the additive on membrane morphology and surface properties.

s0085 3.5.6.1 Inorganic additives

p0255 Inorganic additives can be divided into two major groups: inorganic salts and nanomaterials (metal/metal oxides, e.g., copper, zinc, titania, alumina, and iron oxide, carbon-based nanomaterials, e.g., carbon nanotubes, graphenes, carbon nanofibers, fullerene, and minerals, e.g., clay and zeolites). It is found that inorganic salts like KF, $KMnO_4$, KCl, $ZnCl_2$, KBr, and $NaIO_4$ can influence the interaction among polymer chains and dope quality [117]. During solidification of the membrane in aqueous media, the dispersed salts are leached out from the membrane framework and leave pores behind. For instance, LiCl is a nonsolvent for a PVDF casting solution; hence it leads to the thermodynamic instability of the dope solution and consequently accelerates the liquid–liquid separation [118–121].

p0260 Inorganic nanomaterials are found to diminish finger-like pore formation and hence improve the mechanical strength of polymer membranes. Typically, adding these nanomaterials to the dope solution increases dope viscosity. High viscosity usually acts as a void-suppressing factor; in such a way that it causes a relocation of the composition pathway from an immediate demixing to the delayed one [122–127].

s0090 3.5.6.2 Organic additives

p0265 Two known groups of low- and high-molecular-weight organic additives can either suppress or promote macrovoid formation based on their concentration in the dope solution. The most frequently used low molecular weight organic additives are glycerol (GLY), alcohols, and diols [128], whereas the most commonly used high molecular weight organic additives are polyvinylpyrrolidone (PVP) [40] and polyethylene glycol (PEG) [98,100]. Generally, the addition of the additives mentioned above can improve pore formation, enhance pore interconnectivity, and increase membrane hydrophilicity. For instance, PVP suppresses the finger-like macrovoids formation by getting entrapped in polymer chains and exposing some

hydrophilic character [129]. Also, PEG acts as a pore former. In other words, increasing the concentration of PEG in the dope solution makes the dope thermodynamically less stable, leading to a more porous surface layer [130]. In addition to polymeric additives, organic nanomaterials such as cellulose nanocrystals (CNC) and porous organic frameworks (POF) are used as additives to improve the antifouling and antibacterial properties of phase inversion membranes [131].

3.6 Casting conditions

3.6.1 Evaporation time, temperature, and relative humidity

When there is a certain amount of a volatile solvent or cosolvents in the dope solution, evaporation time can be regulated to achieve a dense membrane surface [96]. During evaporation, the volatile solvent or cosolvent can be removed from the polymeric film, leading to a polymer-concentrated skin layer. Upon immersing in the nonsolvent bath, the concentrated skin layer acts as a resistance between the bulk of the membrane and the nonsolvent bath. This phenomenon prevents in-diffusion of nonsolvent and the out-diffusion of solvent, which results in delayed demixing [32,33].

The temperature of the nonsolvent used for precipitation of the cast film is also important. Generally, precipitation at low temperatures slows down mass diffusion rate, making denser membranes with lower flux and more retentive properties. For this reason, chilled water is frequently used to fabricate CA reverse osmosis membranes [90].

Also, at relatively high humidity in lab-scale synthesis, water droplets could condense on the skin layer where the endothermic cosolvent evaporation decreases the temperature of the membrane film [132]. This may even shift the NIPS process to the VIPS, resulting in symmetric, highly porous membranes with no skin layer.

3.6.2 Sub-layer material

The type of the applied sub-layer greatly affects the demixing rate, particularly in the fabrication of the flat sheet membranes by the NIPS process. Nonwoven fabrics, mica [133], glass [134] or polymeric plates, and metal [133] are usually applied as sub-layer in industrial or lab-scale membrane fabrications. When the support material is nonpermeable, nonsolvent can only penetrate from the top side of a polymeric film into the membrane film during solvent/nonsolvent exchange. It is worth noting that wetting the sub-layer during solvent/nonsolvent exchange does not influence the selective layer morphology, but it could change the support structure. On an industrial scale, when a membrane is fabricated utilizing automatic continuous casting devices, the rear side of the support is in contact with a nonsolvent, which allows the simultaneous solidification from both sides. Wettability of the support material depends on its average pore size, the polymer nature, and so on.

3.6.3 Casting type and speed

Doctor Blade and slot die casting of polymer solution are two primary film casting methods in both lab and industrial scales [135]. However, slot die casting is more suitable than doctor blade casting for continuous casting of a well-developed film, and therefore, this method is commonly used to manufacture polymer films on an industrial scale. In the

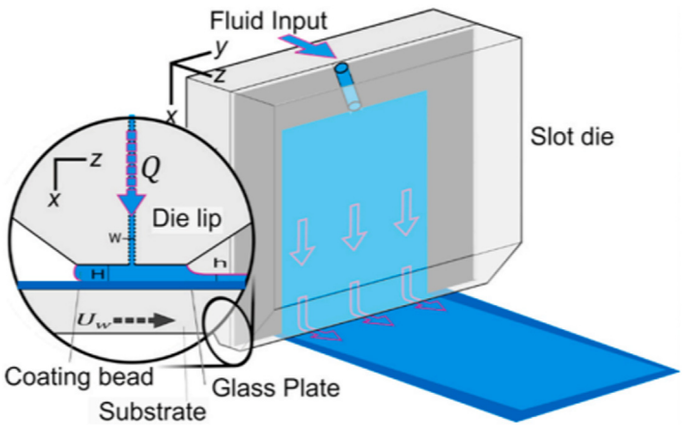

FIGURE 1.14 Schematic of slot die casting device [135]. f0075

slot die casting process, a slot die, as shown in Fig. 1.13A, is used to deposit a polymer solution onto a nonwoven moving substrate at a constant velocity, forming a uniform and precise film on the substrate. The formulation and solution dosing can be premetered by the slot die casting method, making this casting method more flexible than doctor blade casting in terms of providing a wide range of film thickness. In the coating industry, it would be desirable to increase the speed of processing while preserving cast film thickness to maintain the performance of the membrane at a high level, but it might cause to fail to balance these critical factors, such as processing speed and flow rate of casting solution, leading to form some defects on resulting films (Fig. 1.14).

p0295 Due to the existence of the boundary layer at the polymeric film interface, the casting blade speed would affect the membrane structure by changing the polymer molecules' conformation via changing share force rate [136]. During the high-speed casting, the polymer molecules would not have enough time to relax, so shear-induced molecular orientation will be maintained in the nascent skin layer of the membrane, forming a porous membrane with a denser skin layer. As discussed earlier, the formation of a dense layer rapidly at the surface boosts finger-like pore formation due to slowing down the entry of water into the underlaying solution layers. Moreover, the thickness of the skin layer decreases when the shear rate increases, increasing the membrane's permeability [136].

s0115 4. New generation of NIPS membranes

s0120 4.1 Hydrogel-facilitated phase separation membranes

p0300 Hydrogel-facilitated phase separation (HFPS) technique has recently been applied to fabricate the porous membranes by modified NIPS processes [137,138]. In HFPS, a soft lithographically patterned hydrogel mold is used as a water content source that can initiate the phase inversion process. Hydrogels are cross-linked polymers that can maintain a high amount of

water due to their 3D network structure. These highly water-saturated hydrogels can act as a nonsolvent bath. By uniform casting a polymeric solution on top of a hydrogel mold, phase separation initiates immediately (Fig. 1.15). The hydrogel, as a water-based mold, can be easily fabricated with different geometries. The limitations of phase inversion micromolding (PSμM, see Section 4.3) and nanoimprint lithography (NIL) techniques include patterning the nonactive side of the membrane and damaging the membrane's internal structure, respectively, which can be resolved by using the HFPS technique. The membrane's active surface area will also be larger than the equivalent flat surface, and as a result, the membrane performance in terms of water flux will be enhanced without significantly changing the properties of the membrane surface. The morphological properties of the HFPS membranes are almost similar to the membranes prepared with the conventional NIPS process. As shown in Fig. 1.15, the HFPS-fabricated membranes have an asymmetric structure containing finger-like pores on the bottom and a dense skin layer on top [139]. However, pore enlargement exists in the HFPS membranes due to the slow demixing rate between the solvent and nonsolvent during the phase inversion process. Since the concentration gradients of the mold filled with nonsolvent and solvent/polymer mixture are smaller, a delayed phase inversion process is carried out, resulting in membranes with a different performance from each

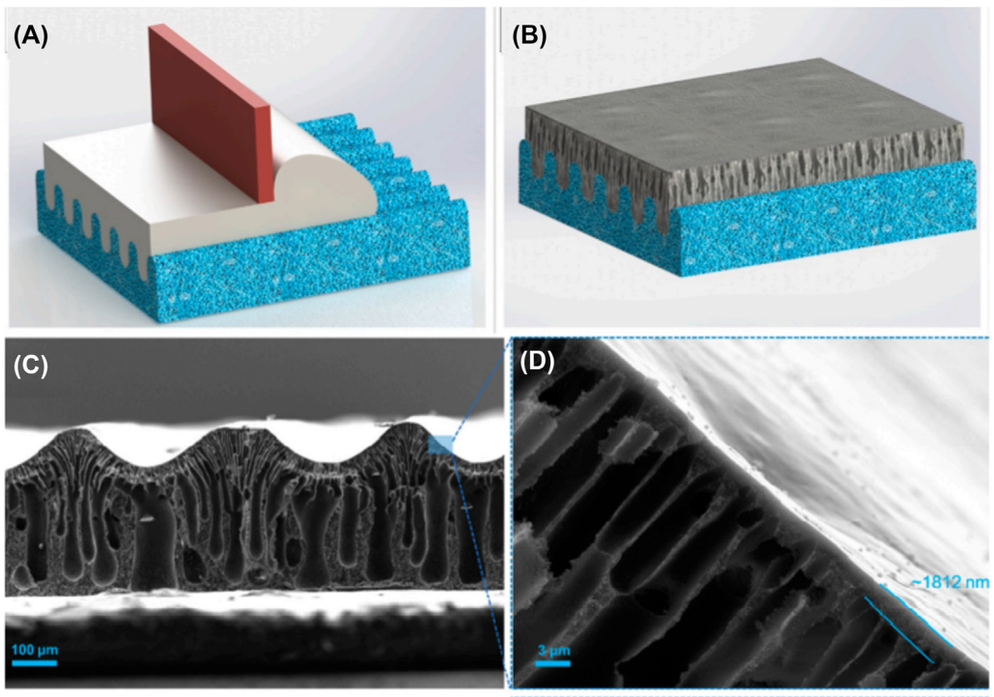

f0080 **FIGURE 1.15** Schematic illustration of the patterned membrane. (A) The hydrogel mold was placed on a glass plate, (B) a polymer solution cast on top hydrogel mold, and (C) cross-section scanning electron microscopy (SEM) images of the patterned membrane at different magnification [138].

casting. The hydrogel content in the mold varies due to the solvent diffusion into the hydrogel from the original membrane cast solution. The continuous use of the mold in repeated membrane casts is limited due to the absorption of solvent into the hydrogel mold, which constrains its practical application. Therefore, the reusability of the hydrogel mold is of interest to lower the cost and time required for large-scale membrane fabrication.

s0125 4.2 Block copolymer self-assembly integrated with nonsolvent induced phase inversion

p0305 Isoporous membranes with uniform and packed pore arrays, as possible next-generation filtration membranes, are expected to solve the trade-off effect between permeability and selectivity problem of conventional NIPS membranes, which provide both high rejection and large permeability [140]. Block copolymers (BCPs) are desired materials to fabricate the isoporous membranes because they spontaneously assemble into periodic nanostructures that can be used to create uniform channels (Fig. 1.16A). These types of membranes are mainly fabricated from the annealed thin film followed by degrading or swelling to prepare permeable membranes. However, roll-to-roll fabrication of isoporous membranes is challenging. It is not feasible to make the isoporous membranes from the conventional NIPS method by simply replacing the polymer with BCPs. Also, a few polymers can be used to make membranes by the approach mentioned above. Therefore, scalable production of isoporous membranes is still a big problem. To overcome this challenge, the block copolymer self-

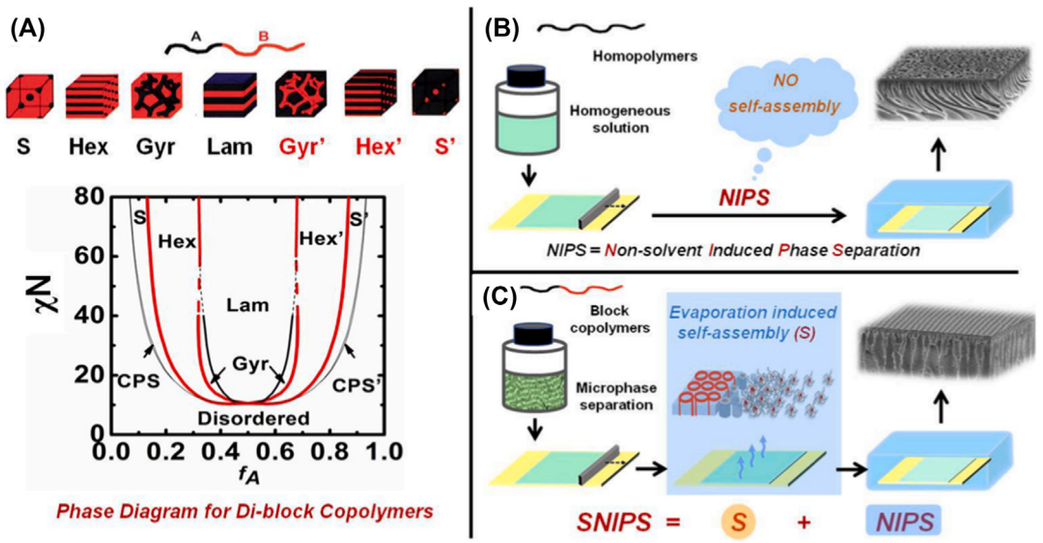

f0085 FIGURE 1.16 (A) Phase diagram and nanostructures created from block copolymers. *S*, spherical; *Hex*, hexagonal; *Gyr*, gyroid; and *Lam*, lamellar. (B) Conventional nonsolvent-induced phase separation (NIPS) process and asymmetric membranes fabricated from homopolymers; and (C) self-assembly nonsolvent-induced phase separation (SNIPS) process and the asymmetric isoporous membranes fabricated from block copolymers [141].

assembly (S) is combined with the conventional NIPS process Fig. 1.16B and C, which is called SNIPS, as proposed by Peinemann and Abetz in 2007 [142]. This integrated SNIPS approach provides many advantages due to its easy operation and high compatibility with roll-to-roll production. Isoporous membranes produced from SNIPS also demonstrate a typical integrated asymmetric structure, consisting of an isoporous top surface and a gradient sublayer. This asymmetric structure created through SNIPS approach is consistent with the concepts of both BCPs self-assembly and NIPS process. It enables this approach to independently regulate the surface and internal porosity, which are important for fast transport and precise separation. The mechanism of isopores generation on membranes through the SNIPS process is based on the block copolymers micellization dissolved in the casting solution [143]. Different types of isoporous membrane configurations, that is, composite, flat sheet, and hollow fibers, can be prepared by spinning machines [144], indicating the potential of this newly scalable manufacturing technology in fabricating the isoporous membranes. However, many efforts are still required to (i) improve the structural properties and reproductivity, (ii) mitigate the defect formation, and (iii) decrease the cost of asymmetric isoporous membrane production. Basically, this process initiates from a homogeneous casting solution consisting of BCPs, solvents, and selected additives. For a given BCP, the desired solvent for membrane production can be barely changed. However, the additives in the casting solution provide

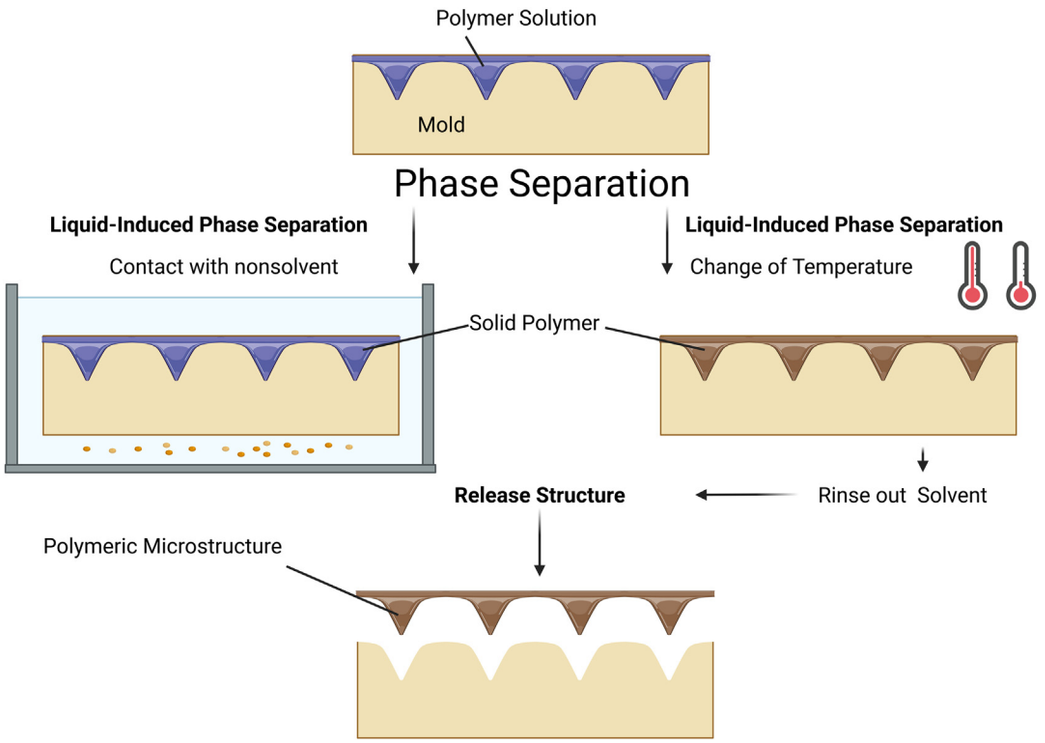

f0090 FIGURE 1.17 Schematic representation of the PSμM process in which a layer of polymer solution is cast on a mold with a micrometer-sized relief profile on the backside of the membrane. Either thermally induced phase separation (TIPS) or nonsolvent-induced phase separation (NIPS) can solidify the cast film. The polymeric solidified microstructure can be easily released from the mold.

numerous opportunities for controlled fabrication as well as surface functionalization, as proved in the NIPS process. The close relationship between SNIPS and NIPS demonstrates that blending strategies is also applicable to fabricating tailored membrane structures via the SNIPS method [12,145].

s0130 4.3 Phase separation micromolding

p0310 Phase separation micromolding (PSμM) is another technique for the fabrication of patterned porous membranes [146–148]. In this method, the polymer solution is cast on the support layer with the desired template, typically a silicon wafer with a recurring design made by photolithography (Fig. 1.17). Then, phase separation begins either by immersing in a coagulation bath (NIPS) or subjecting to humid air (VIPS). The membranes with a patterned surface can be used in various applications such as microfluidic apparatuses, frameworks for tissue engineering, and microsieves [149]. Moreover, micromolding can be applied to fabricate a layer with a two-tier hierarchical structure that shows hydrophobic behavior [150]. Also, the patterned surfaces can be more resistant to the sedimentation of microbial cells [151,152]. Nevertheless, the main challenge of the PSμM method is that the skin layer, which is in direct contact with the wastewater and is responsible for the selective properties of the membrane, is not patterned.

s0135 4.4 Breath-figure technique to make honeycomb configuration

p0315 A membrane possessing a honeycomb configuration, a 2D set of hexagonal pores, can be synthesized through rapid solvent vapourization in moist air along with water drop

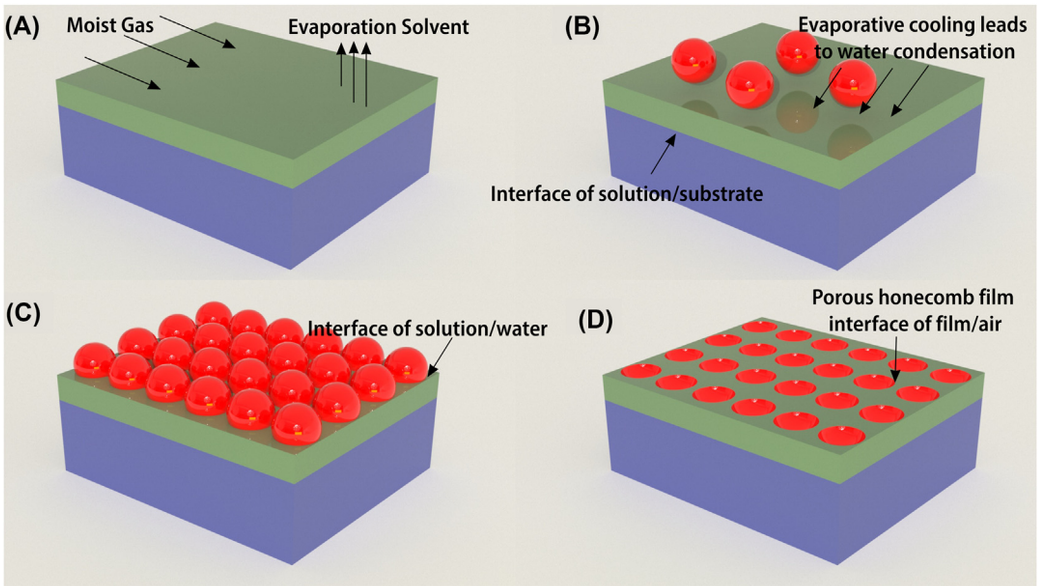

f0095 FIGURE 1.18 Schematic representation of the formation of honeycomb films by breath-figure technique. (A) solvent vapourization in contact with moist air, (B) water condensation on top of the film, (C) solvent-nonsolvent demixing, and (D) formation of porous honeycomb film a the interface if film/air.

condensation [153–156]. The applied solvent must be volatile and immiscible with water. Condensation of water vapor occurs due to the reduction of the surface temperature induced by solvent vapourization. Then, phase inversion takes place on the skin layer due to the immiscibility of the solvent with water, resulting in the growth of the nuclei of water drops which convert to hexagonal pores (Fig. 1.18). Although the breath-figure technique is rarely applied to fabricate porous membranes, since the hexagonal pores are not through-pores across the layers, casting a polymeric film on an ice substrate leads to forming a porous structure, making this technique still viable [157–159].

s0140

5. Conclusion

p0320 In this chapter, the basic description, principles, and fundamental mechanisms of the nonsolvent-induced phase inversion process for the fabrication of porous and asymmetric membranes were discussed. The mechanism of macrovoids formation and the trade-off between thermodynamic and kinetic parameters to fabricate desired membranes were presented in detail. This interplay can provide valuable insight into the critical processing parameters in manufacturing membranes, including the type of solvent-nonsolvent pairs, type of polymer, the composition of the polymer solution and the coagulation bath, the type of additives for the casting solution, and film casting conditions. The fundamental principles demonstrated in this chapter can be used as guidelines to adjust the main factors involved in membrane formation to fabricate phase inversion membranes with desired morphology and separation performances. The last part of this chapter provides the new trends in fabricating next-generation phase inversion membranes. While endowing the conventional NIPS membranes with some advantages (such as increased surface area and uniform pore size), these novel methods still suffer from several inherent challenges that can be the focus of many future research works.

References

[1] E. Zolghadr, M.D. Firouzjaei, G. Amouzandeh, P. LeClair, M. Elliott, The role of membrane-based technologies in environmental treatment and reuse of produced water, Frontiers in Environmental Science 9 (2021), https://doi.org/10.3389/fenvs.2021.629767.

[2] A. Rahimpour, S.F. Seyedpour, S. Aghapour Aktij, M. Dadashi Firouzjaei, A. Zirehpour, A. Arabi Shamsabadi, S. Khoshhal Salestan, M. Jabbari, M. Soroush, Simultaneous improvement of antimicrobial, antifouling, and transport properties of forward osmosis membranes with immobilized highly-compatible polyrhodanine nanoparticles, Environmental Science & Technology 52 (9) (2018) 5246–5258.

[3] P. Karami, S.A. Aktij, B. Khorshidi, M.D. Firouzjaei, A. Asad, M. Elliott, A. Rahimpour, J.B.P. Soares, M. Sadrzadeh, Nanodiamond-decorated thin film composite membranes with antifouling and antibacterial properties, Desalination 522 (2022) 115436, https://doi.org/10.1016/j.desal.2021.115436.

[4] M. Dadashi Firouzjaei, M. Karimiziarani, H. Moradkhani, M. Elliott, B. Anasori, MXenes: the two-dimensional influencers, Materials Today Advances 13 (2022) 100202, https://doi.org/10.1016/j.mtadv.2021.100202.

[5] E. Zolghadr, M. Dadashi Firouzjaei, S. Aghapour Aktij, A. Aghaei, E.K. Wujcik, M. Sadrzadeh, A. Rahimpour, F.A. Afkhami, P. LeClair, M. Elliott, An ultrasonic-assisted rapid approach for sustainable fabrication of antibacterial and anti-biofouling membranes via metal-organic frameworks, Materials Today Chemistry 26 (2022) 101044, https://doi.org/10.1016/j.mtchem.2022.101044.

[6] M. Dadashi Firouzjaei, E. Zolghadr, S. Ahmadalipour, N. Taghvaei, F. Akbari Afkhami, S. Nejati, M.A. Elliott, Chemistry, abundance, detection and treatment of per- and polyfluoroalkyl substances in water: a review, Environmental Chemistry Letters 20 (1) (2022) 661–679, https://doi.org/10.1007/s10311-021-01340-6.

[7] S. Madaeni, A. Rahimpour, Effect of type of solvent and non-solvents on morphology and performance of polysulfone and polyethersulfone ultrafiltration membranes for milk concentration, Polymers for Advanced Technologies 16 (10) (2005) 717–724.
[8] H. Jafarian, M. Dadashi Firouzjaei, S. Aghapour Aktij, A. Aghaei, M. Pilevar Khomami, M. Elliott, E.K. Wujcik, M. Sadrzadeh, A. Rahimpour, Synthesis of heterogeneous metal organic Framework-Graphene oxide nanocomposite membranes for water treatment, Chemical Engineering Journal 455 (2023) 140851, https://doi.org/10.1016/j.cej.2022.140851.
[9] S. Mohammad Nejad, S.F. Seyedpour, S. Aghapour Aktij, M. Dadashi Firouzjaei, M. Elliott, A. Tiraferri, M. Sadrzadeh, A. Rahimpour, Loose nanofiltration membranes functionalized with in situ-synthesized metal organic framework for water treatment, Materials Today Chemistry 24 (2022) 100909, https://doi.org/10.1016/j.mtchem.2022.100909.
[10] M.D. Firouzjaei, Environmental Application of Two-and Three-Dimensional Nanomaterials for Wastewater Treatment, University of Alabama Libraries, 2022.
[11] M.D. Firouzjaei, The Water Purification Robustness of Metal-Organic Framework-Polyamide Nanocomposite Thin Films Toward Long Term Organic, Inorganic, and Bacterial Contamination, University of Alabama Libraries, 2020.
[12] M. Pejman, M. Dadashi Firouzjaei, S. Aghapour Aktij, E. Zolghadr, P. Das, M. Elliott, M. Sadrzadeh, M. Sangermano, A. Rahimpour, A. Tiraferri, Effective strategy for UV-mediated grafting of biocidal Ag-MOFs on polymeric membranes aimed at enhanced water ultrafiltration, Chemical Engineering Journal 426 (2021) 130704, https://doi.org/10.1016/j.cej.2021.130704.
[13] M. Mulder, Preparation of Synthetic Membranes, Basic Principles of Membrane Technology, Springer, 1996, pp. 71–156.
[14] M. Peyravi, A. Rahimpour, M. Jahanshahi, A. Javadi, A. Shockravi, Tailoring the surface properties of PES ultrafiltration membranes to reduce the fouling resistance using synthesized hydrophilic copolymer, Microporous and Mesoporous Materials 160 (2012) 114–125.
[15] M.R. Esfahani, S.A. Aktij, Z. Dabaghian, M.D. Firouzjaei, A. Rahimpour, J. Eke, I.C. Escobar, M. Abolhassani, L.F. Greenlee, A.R. Esfahani, Nanocomposite membranes for water separation and purification: fabrication, modification, and applications, Separation and Purification Technology 213 (2019) 465–499, https://doi.org/10.1016/j.seppur.2018.12.050.
[16] M. Pejman, M.D. Firouzjaei, S.A. Aktij, P. Das, E. Zolghadr, H. Jafarian, A.A. Shamsabadi, M. Elliott, M.R. Esfahani, M. Sangermano, M. Sadrzadeh, E.K. Wujcik, A. Rahimpour, A. Tiraferri, Improved antifouling and antibacterial properties of forward osmosis membranes through surface modification with zwitterions and silver-based metal organic frameworks, Journal of Membrane Science 611 (2020) 118352, https://doi.org/10.1016/j.memsci.2020.118352.
[17] A. Aghaei, M.D. Firouzjaei, P. Karami, S.A. Aktij, M. Elliott, Y. Mansourpanah, A. Rahimpour, J.B.P. Soares, M. Sadrzadeh, The implications of 3D-printed membranes for water and wastewater treatment and resource recovery, Canadian Journal of Chemical Engineering 100 (9) (2022) 2309–2321, https://doi.org/10.1002/cjce.24488.
[18] A. Rahimpour, S. Madaeni, S. Zereshki, Y. Mansourpanah, Preparation and characterization of modified nanoporous PVDF membrane with high antifouling property using UV photo-grafting, Applied Surface Science 255 (16) (2009) 7455–7461.
[19] A. Rahimpour, S.S. Madaeni, S. Ghorbani, A. Shockravi, Y. Mansourpanah, The influence of sulfonated polyethersulfone (SPES) on surface nano-morphology and performance of polyethersulfone (PES) membrane, Applied Surface Science 256 (6) (2010) 1825–1831.
[20] S.F. Seyedpour, M. Dadashi Firouzjaei, A. Rahimpour, E. Zolghadr, A. Arabi Shamsabadi, P. Das, F. Akbari Afkhami, M. Sadrzadeh, A. Tiraferri, M. Elliott, Toward sustainable tackling of biofouling implications and improved performance of TFC FO membranes modified by Ag-MOF nanorods, ACS Applied Materials & Interfaces 12 (34) (2020) 38285–38298, https://doi.org/10.1021/acsami.0c13029.
[21] M. Mozafari, S.F. Seyedpour, S.K. Salestan, A. Rahimpour, A.A. Shamsabadi, M.D. Firouzjaei, M.R. Esfahani, A. Tiraferri, H. Mohsenian, M. Sangermano, M. Soroush, Facile Cu-BTC surface modification of thin chitosan film coated polyethersulfone membranes with improved antifouling properties for sustainable removal of manganese, Journal of Membrane Science 588 (2019) 117200, https://doi.org/10.1016/j.memsci.2019.117200.

[22] M. Pejman, M. Dadashi Firouzjaei, S. Aghapour Aktij, P. Das, E. Zolghadr, H. Jafarian, A. Arabi Shamsabadi, M. Elliott, M. Sadrzadeh, M. Sangermano, A. Rahimpour, A. Tiraferri, In situ Ag-MOF growth on pre-grafted zwitterions imparts outstanding antifouling properties to forward osmosis membranes, ACS Applied Materials & Interfaces 12 (32) (2020) 36287–36300, https://doi.org/10.1021/acsami.0c12141.
[23] M.R.S. Kebria, A. Rahimpour, Membrane Distillation: Basics, Advances, and Applications, Advances in Membrane Technologies, IntechOpen, 2020.
[24] Y. Mansourpanah, S. Madaeni, A. Rahimpour, M. Adeli, M. Hashemi, M. Moradian, Fabrication new PES-based mixed matrix nanocomposite membranes using polycaprolactone modified carbon nanotubes as the additive: property changes and morphological studies, Desalination 277 (1–3) (2011) 171–177.
[25] S. Loeb, S. Sourirajan, Sea Water Demineralization by Means of an Osmotic Membrane, ACS Publications, 1962.
[26] A. Rahimpour, M. Jahanshahi, A. Mollahosseini, B. Rajaeian, Structural and performance properties of UV-assisted TiO2 deposited nano-composite PVDF/SPES membranes, Desalination 285 (2012) 31–38.
[27] A. Rahimpour, S. Madaeni, S. Mehdipour-Ataei, Synthesis of a novel poly (amide-imide)(PAI) and preparation and characterization of PAI blended polyethersulfone (PES) membranes, Journal of Membrane Science 311 (1–2) (2008) 349–359.
[28] A. Rahimpour, S. Madaeni, A. Shockravi, S. Ghorbani, Preparation and characterization of hydrophile nano-porous polyethersulfone membranes using synthesized poly (sulfoxide-amide) as additive in the casting solution, Journal of Membrane Science 334 (1–2) (2009) 64–73.
[29] A.K. Ghosh, B.-H. Jeong, X. Huang, E.M. Hoek, Impacts of reaction and curing conditions on polyamide composite reverse osmosis membrane properties, Journal of Membrane Science 311 (1–2) (2008) 34–45.
[30] A. Rahimpour, S.S. Madaeni, Polyethersulfone (PES)/cellulose acetate phthalate (CAP) blend ultrafiltration membranes: preparation, morphology, performance and antifouling properties, Journal of Membrane Science 305 (1–2) (2007) 299–312.
[31] A. Rahimpour, UV photo-grafting of hydrophilic monomers onto the surface of nano-porous PES membranes for improving surface properties, Desalination 265 (1–3) (2011) 93–101.
[32] P. Vandezande, L.E. Gevers, I.F. Vankelecom, Solvent resistant nanofiltration: separating on a molecular level, Chemical Society Reviews 37 (2) (2008) 365–405.
[33] I. Vankelecom, K. De Smet, L. Gevers, P. Jacobs, Nanofiltration membrane materials and preparation, in: A. Schaefer, A. Fane, A. Waite (Eds.), Nanofiltration: Principles and Applications, Elsevier, Oxford, UK, 2005, pp. 33–65.
[34] A. Fane, C. Tang, R. Wang, Membrane Technology for Water: Microfiltration, Ultrafiltration, Nanofiltration, and Reverse Osmosis, 2011.
[35] M.A. Frommer, D. Lancet, The Mechanism of Membrane Formation: Membrane Structures and Their Relation to Preparation Conditions, Reverse Osmosis Membrane Research, Springer, 1972, pp. 85–110.
[36] H. Strathmann, K. Kock, P. Amar, R. Baker, The formation mechanism of asymmetric membranes, Desalination 16 (2) (1975) 179–203.
[37] D.-M. Wang, F.-C. Lin, J.-C. Chiang, J.-Y. Lai, Control of the porosity of asymmetric TPX membranes, Journal of Membrane Science 141 (1) (1998) 1–12.
[38] A.K. Hołda, B. Aernouts, W. Saeys, I.F. Vankelecom, Study of polymer concentration and evaporation time as phase inversion parameters for polysulfone-based SRNF membranes, Journal of Membrane Science 442 (2013) 196–205.
[39] K. Kimmerle, H. Strathmann, Analysis of the structure-determining process of phase inversion membranes, Desalination 79 (2–3) (1990) 283–302.
[40] R. Boom, I. Wienk, T. Van den Boomgaard, C. Smolders, Microstructures in phase inversion membranes. Part 2. The role of a polymeric additive, Journal of Membrane Science 73 (2–3) (1992) 277–292.
[41] M.R.S. Kebria, M. Jahanshahi, A. Rahimpour, SiO2 modified polyethyleneimine-based nanofiltration membranes for dye removal from aqueous and organic solutions, Desalination 367 (2015) 255–264.
[42] M. Sadrzadeh, S. Bhattacharjee, Rational design of phase inversion membranes by tailoring thermodynamics and kinetics of casting solution using polymer additives, Journal of Membrane Science 441 (2013) 31–44.
[43] T. Ahmad, C. Guria, A. Mandal, Kinetic modeling and simulation of non-solvent induced phase separation: immersion precipitation of PVC-based casting solution in a finite salt coagulation bath, Polymer 199 (2020) 122527.

[44] C.M. Hansen, Three dimensional solubility parameter-key to paint-component affinities: dyes, emulsifiers, mutual solubility and compatibility, and pigments, Journal of Paint Technology 39 (1967) 505.
[45] R.F. Blanks, J. Prausnitz, Thermodynamics of polymer solubility in polar and nonpolar systems, Industrial & Engineering Chemistry Fundamentals 3 (1) (1964) 1–8.
[46] Q. Wang, Z. Wang, Z. Wu, Effects of solvent compositions on physicochemical properties and anti-fouling ability of PVDF microfiltration membranes for wastewater treatment, Desalination 297 (2012) 79–86.
[47] R.J. Ray, W.B. Krantz, R.L. Sani, Linear stability theory model for finger formation in asymmetric membranes, Journal of Membrane Science 23 (2) (1985) 155–182.
[48] C. Smolders, A. Reuvers, R. Boom, I. Wienk, Microstructures in phase-inversion membranes. Part 1. Formation of macrovoids, Journal of Membrane Science 73 (2–3) (1992) 259–275.
[49] W.-L. Hung, D.-M. Wang, J.-Y. Lai, S.-C. Chou, On the initiation of macrovoids in polymeric membranes–effect of polymer chain entanglement, Journal of Membrane Science 505 (2016) 70–81.
[50] H. Matsuyama, T. Maki, M. Teramoto, K. Kobayashi, Effect of PVP additive on porous polysulfone membrane formation by immersion precipitation method, Separation Science and Technology 38 (14) (2003) 3449–3458.
[51] L. Yilmaz, A. McHugh, Modelling of asymmetric membrane formation. I. Critique of evaporation models and development of a diffusion equation formalism for the quench period, Journal of Membrane Science 28 (3) (1986) 287–310.
[52] M. Ulbricht, Advanced functional polymer membranes, Polymer 47 (7) (2006) 2217–2262.
[53] I.C. Kim, H.G. Yoon, K.H. Lee, Formation of integrally skinned asymmetric polyetherimide nanofiltration membranes by phase inversion process, Journal of Applied Polymer Science 84 (6) (2002) 1300–1307.
[54] H. Kim, R. Tyagi, A. Fouda, K. Ionasson, The kinetic study for asymmetric membrane formation via phase-inversion process, Journal of Applied Polymer Science 62 (4) (1996) 621–629.
[55] S. Madaeni, N.T. Hasankiadeh, A. Kurdian, A. Rahimpour, Modeling and optimization of membrane fabrication using artificial neural network and genetic algorithm, Separation and Purification Technology 76 (1) (2010) 33–43.
[56] Y. Mansourpanah, S. Madaeni, A. Rahimpour, Z. Kheirollahi, M. Adeli, Changing the performance and morphology of polyethersulfone/polyimide blend nanofiltration membranes using trimethylamine, Desalination 256 (1–3) (2010) 101–107.
[57] A. Rahimpour, S. Madaeni, Y. Mansourpanah, High performance polyethersulfone UF membrane for manufacturing spiral wound module: preparation, morphology, performance, and chemical cleaning, Polymers for Advanced Technologies 18 (5) (2007) 403–410.
[58] S. Madaeni, A. Rahimpour, A. Ghaedi, Effect of solvent on morphology and performance of polysulfone and polyethersulfone ultrafiltration membranes for milk concentration, Technology 23 (2004) 25.
[59] M.R.S. Kebria, A. Rahimpour, S.K. Salestan, S.F. Seyedpour, A. Jafari, F. Banisheykholeslami, N.T.H. Kiadeh, Hyper-branched dendritic structure modified PVDF electrospun membranes for air gap membrane distillation, Desalination 479 (2020) 114307.
[60] A. Mousavinejad, A. Rahimpour, M.R. Shirzad Kebria, S. Khoshhal Salestan, M. Sadrzadeh, N. Tavajohi, A Nickel-Based Metal Organic Framework to Improve the CO2/CH4 Separation Capability of Thin Film Pebax Membranes, Industrial & Engineering Chemistry Research, 2020.
[61] M. Mazani, S. Aghapour Aktij, A. Rahimpour, N. Tavajohi Hassan Kiadeh, Cu-BTC Metal– organic framework modified membranes for landfill leachate treatment, Water 12 (1) (2020) 91.
[62] P.J. Flory, Thermodynamics of high polymer solutions, The Journal of Chemical Physics 10 (1) (1942) 51–61.
[63] M.L. Huggins, Solutions of long chain compounds, The Journal of Chemical Physics 9 (5) (1941) 440.
[64] M.L. Huggins, Theory of solutions of high polymers1, Journal of the American Chemical Society 64 (7) (1942) 1712–1719.
[65] J.R. Fried, Polymer Science and Technology, Prentice Hall, Upper Saddle River, NJ, 2003.
[66] P. Flory, W. Krigbaum, Statistical mechanics of dilute polymer solutions. II, The Journal of Chemical Physics 18 (8) (1950) 1086–1094.
[67] R. Koningsveld, L. Kleintjens, H. Schoffeleers, Thermodynamic Aspects of Polymer Compatibility, Macromolecular Chemistry–9, Elsevier, 1974, pp. 1–32.
[68] G.R. Guillen, Y. Pan, M. Li, E.M. Hoek, Preparation and characterization of membranes formed by nonsolvent induced phase separation: a review, Industrial & Engineering Chemistry Research 50 (7) (2011) 3798–3817.

[69] M.S. Kebria, A. Rahimpour, R. Abedini, Preparation and characterisation of new microporous Elvaloy4170 coated PVDF membrane for desalination by air gap membrane distillation, Micro & Nano Letters 14 (5) (2019) 551–555.
[70] M.G. Yusefi, A. Rahimpour, H. Mehdipour, Hydrophobic modification of PVDF membranes for biodiesel purification, Biofuels 7 (3) (2016) 263–270.
[71] A. Aghaei, K. Suresh, M.D. Firouzjaei, M. Elliott, A. Rahimpour, M. Sadrzadeh, 14: Hybrid/integrated treatment technologies for oily wastewater treatment, in: A. Basile, A. Cassano, M.R. Rahimpour, M.A. Makarem (Eds.), Advanced Technologies in Wastewater Treatment, Elsevier, 2023, pp. 377–419, https://doi.org/10.1016/B978-0-323-99916-8.00002-X.
[72] S. Pourjafar, M. Jahanshahi, A. Rahimpour, Optimization of TiO2 modified poly (vinyl alcohol) thin film composite nanofiltration membranes using Taguchi method, Desalination 315 (2013) 107–114.
[73] A. Rahimpour, Preparation and modification of nano-porous polyimide (PI) membranes by UV photo-grafting process: ultrafiltration and nanofiltration performance, Korean Journal of Chemical Engineering 28 (1) (2011) 261–266.
[74] S.F. Seyedpour, A. Rahimpour, H. Mohsenian, M.J. Taherzadeh, Low fouling ultrathin nanocomposite membranes for efficient removal of manganese, Journal of Membrane Science 549 (2018) 205–216.
[75] S.A. Aktij, A. Rahimpour, A. Figoli, Low content nano-polyrhodanine modified polysulfone membranes with superior properties and their performance for wastewater treatment, Environmental Science: Nano 4 (10) (2017) 2043–2054.
[76] M.D. Firouzjaei, A.A. Shamsabadi, S.A. Aktij, S.F. Seyedpour, M. Sharifian Gh, A. Rahimpour, M.R. Esfahani, M. Ulbricht, M. Soroush, Exploiting synergetic effects of graphene oxide and a silver-based metal–organic framework to enhance antifouling and anti-biofouling properties of thin-film nanocomposite membranes, ACS Applied Materials & Interfaces 10 (49) (2018) 42967–42978.
[77] M.D. Firouzjaei, S.F. Seyedpour, S.A. Aktij, M. Giagnorio, N. Bazrafshan, A. Mollahosseini, F. Samadi, S. Ahmadalipour, F.D. Firouzjaei, M.R. Esfahani, Recent advances in functionalized polymer membranes for biofouling control and mitigation in forward osmosis, Journal of Membrane Science 596 (2020) 117604.
[78] M. Pejman, M. Dadashi Firouzjaei, S. Aghapour Aktij, P. Das, E. Zolghadr, H. Jafarian, A. Arabi Shamsabadi, M.A. Elliott, M. Sadrzadeh, M. Sangermano, In-Situ Ag-MOFs Growth on Pre-grafted Zwitterions Imparts Outstanding Antifouling Properties to Forward Osmosis Membranes, ACS Applied Materials & Interfaces, 2020.
[79] S. Noamani, S. Niroomand, M. Rastgar, A. McDonald, M. Sadrzadeh, Development of a self-sustained model to predict the performance of direct contact membrane distillation, Separation and Purification Technology 263 (2021) 118407.
[80] S. Noamani, M. Sadrzadeh, A.R. Tehrani-Bagha, Prospects of Nanocomposite Membranes for Water Treatment by Membrane Distillation, Nanocomposite Membranes for Water and Gas Separation, Elsevier, 2020, pp. 299–320.
[81] M. Dadashi Firouzjaei, E. Zolghadr, A. Arabi Shamsabadi, M. Sadrzadeh, A. Rahimpour, F. Akbari Afkhami, E.K. Wujcik, M. Elliott, Clean water recycling through adsorption via heterogeneous nanocomposites: silver-based metal-organic framework embellished with graphene oxide and MXene, Case Studies in Chemical and Environmental Engineering 7 (2023) 100296, https://doi.org/10.1016/j.cscee.2023.100296.
[82] A. Zirehpour, A. Rahimpour, F. Seyedpour, M. Jahanshahi, Developing new CTA/CA-based membrane containing hydrophilic nanoparticles to enhance the forward osmosis desalination, Desalination 371 (2015) 46–57.
[83] M.R.S. Kebria, A. Rahimpour, G. Bakeri, R. Abedini, Experimental and theoretical investigation of thin ZIF-8/chitosan coated layer on air gap membrane distillation performance of PVDF membrane, Desalination 450 (2019) 21–32.
[84] A. Mehrparvar, A. Rahimpour, Surface modification of novel polyether sulfone amide (PESA) ultrafiltration membranes by grafting hydrophilic monomers, Journal of Industrial and Engineering Chemistry 28 (2015) 359–368.
[85] R.W. Baker, Membrane Technology and Applications, John Wiley & Sons, New York, 2012.
[86] D. Mosqueda-Jimenez, R. Narbaitz, T. Matsuura, G. Chowdhury, G. Pleizier, J. Santerre, Influence of processing conditions on the properties of ultrafiltration membranes, Journal of Membrane Science 231 (1–2) (2004) 209–224.

[87] L.-W. Chen, T.-H. Young, Effect of nonsolvents on the mechanism of wet-casting membrane formation from EVAL copolymers, Journal of Membrane Science 59 (1) (1991) 15–26.
[88] M.-J. Han, D. Bhattacharyya, Morphology and transport study of phase inversion polysulfone membranes, Chemical Engineering Communications 128 (1) (1994) 197–209.
[89] S.K. Yong, J.K. Hyo, Y.K. Un, Asymmetric membrane formation via immersion precipitation method. I. Kinetic effect, Journal of Membrane Science 60 (2–3) (1991) 219–232.
[90] J.T. Jung, J.F. Kim, H.H. Wang, E. di Nicolo, E. Drioli, Y.M. Lee, Understanding the non-solvent induced phase separation (NIPS) effect during the fabrication of microporous PVDF membranes via thermally induced phase separation (TIPS), Journal of Membrane Science 514 (2016) 250–263, https://doi.org/10.1016/j.memsci.2016.04.069.
[91] Q. Ge, L. Ding, T. Wu, G. Xu, F. Yang, M. Xiang, Effect of surfactant on morphology and pore size of polysulfone membrane, Journal of Polymer Research 25 (1) (2018) 21.
[92] P. Sukitpaneenit, T.-S. Chung, Molecular elucidation of morphology and mechanical properties of PVDF hollow fiber membranes from aspects of phase inversion, crystallization and rheology, Journal of Membrane Science 340 (1–2) (2009) 192–205.
[93] S. Yang, Z. Liu, Preparation and characterization of polyacrylonitrile ultrafiltration membranes, Journal of Membrane Science 222 (1–2) (2003) 87–98.
[94] A. Rahimpour, S.S. Madaeni, Y. Mansourpanah, Nano-porous polyethersulfone (PES) membranes modified by acrylic acid (AA) and 2-hydroxyethylmethacrylate (HEMA) as additives in the gelation media, Journal of Membrane Science 364 (1–2) (2010) 380–388.
[95] I. Soroko, M.P. Lopes, A. Livingston, The effect of membrane formation parameters on performance of polyimide membranes for organic solvent nanofiltration (OSN): part A. Effect of polymer/solvent/non-solvent system choice, Journal of Membrane Science 381 (1–2) (2011) 152–162.
[96] P. Vandezande, X. Li, L.E. Gevers, I.F. Vankelecom, High throughput study of phase inversion parameters for polyimide-based SRNF membranes, Journal of Membrane Science 330 (1–2) (2009) 307–318.
[97] I. Soroko, M. Makowski, F. Spill, A. Livingston, The effect of membrane formation parameters on performance of polyimide membranes for organic solvent nanofiltration (OSN). Part B: analysis of evaporation step and the role of a co-solvent, Journal of Membrane Science 381 (1–2) (2011) 163–171.
[98] B. Chakrabarty, A. Ghoshal, M. Purkait, Effect of molecular weight of PEG on membrane morphology and transport properties, Journal of Membrane Science 309 (1–2) (2008) 209–221.
[99] I.-C. Kim, K.-H. Lee, Effect of poly (ethylene glycol) 200 on the formation of a polyetherimide asymmetric membrane and its performance in aqueous solvent mixture permeation, Journal of Membrane Science 230 (1–2) (2004) 183–188.
[100] Y. Ma, F. Shi, J. Ma, M. Wu, J. Zhang, C. Gao, Effect of PEG additive on the morphology and performance of polysulfone ultrafiltration membranes, Desalination 272 (1–3) (2011) 51–58.
[101] Z.-L. Xu, T.-S. Chung, K.-C. Loh, B.C. Lim, Polymeric asymmetric membranes made from polyetherimide/polybenzimidazole/poly (ethylene glycol)(PEI/PBI/PEG) for oil–surfactant–water separation, Journal of Membrane Science 158 (1–2) (1999) 41–53.
[102] M.D. Firouzjaei, S.K. Nemani, M. Sadrzadeh, E.K. Wujcik, M. Elliott, B. Anasori, Life cycle assessment of Ti3C2Tx MXene synthesis, Advanced Materials (2023) 2300422, https://doi.org/10.1002/adma.202300422.
[103] P. Aerts, E. Van Hoof, R. Leysen, I. Vankelecom, P. Jacobs, Polysulfone–Aerosil composite membranes: Part 1. The influence of the addition of Aerosil on the formation process and membrane morphology, Journal of Membrane Science 176 (1) (2000) 63–73.
[104] A. Mollahosseini, A. Rahimpour, M. Jahamshahi, M. Peyravi, M. Khavarpour, The effect of silver nanoparticle size on performance and antibacteriality of polysulfone ultrafiltration membrane, Desalination 306 (2012) 41–50.
[105] M. Peyravi, A. Rahimpour, M. Jahanshahi, Developing nanocomposite PI membranes: morphology and performance to glycerol removal at the downstream processing of biodiesel production, Journal of Membrane Science 473 (2015) 72–84.
[106] F. Seidi, A. Arabi Shamsabadi, M. Dadashi Firouzjaei, M. Elliott, M.R. Saeb, Y. Huang, C. Li, H. Xiao, B. Anasori, MXenes antibacterial properties and applications: a review and perspective, Small 19 (14) (2023) 2206716, https://doi.org/10.1002/smll.202206716.

[107] Y. Rezaeipour, E. Zolghadr, P. Alizadeh, G. Sadri, E.K. Wujcik, F.A. Afkhami, M. Elliott, M. Dadashi Firouzjaei, The anticancer properties of metal-organic frameworks and their heterogeneous nanocomposites, Biomaterials Advances 139 (2022) 213013, https://doi.org/10.1016/j.bioadv.2022.213013.
[108] A. Rahimpour, S. Madaeni, A. Taheri, Y. Mansourpanah, Coupling TiO2 nanoparticles with UV irradiation for modification of polyethersulfone ultrafiltration membranes, Journal of Membrane Science 313 (1–2) (2008) 158–169.
[109] A. Rahimpour, M. Jahanshahi, B. Rajaeian, M. Rahimnejad, TiO2 entrapped nano-composite PVDF/SPES membranes: preparation, characterization, antifouling and antibacterial properties, Desalination 278 (1–3) (2011) 343–353.
[110] A. Rahimpour, M. Jahanshahi, S. Khalili, A. Mollahosseini, A. Zirepour, B. Rajaeian, Novel functionalized carbon nanotubes for improving the surface properties and performance of polyethersulfone (PES) membrane, Desalination 286 (2012) 99–107.
[111] A. Rahimpour, S. Madaeni, Y. Mansourpanah, The effect of anionic, non-ionic and cationic surfactants on morphology and performance of polyethersulfone ultrafiltration membranes for milk concentration, Journal of Membrane Science 296 (1–2) (2007) 110–121.
[112] S. Mokhtari, A. Rahimpour, A.A. Shamsabadi, S. Habibzadeh, M. Soroush, Enhancing performance and surface antifouling properties of polysulfone ultrafiltration membranes with salicylate-alumoxane nanoparticles, Applied Surface Science 393 (2017) 93–102, https://doi.org/10.1016/j.apsusc.2016.10.005.
[113] A. Zirehpour, A. Rahimpour, S. Khoshhal, M.D. Firouzjaei, A.A. Ghoreyshi, The impact of MOF feasibility to improve the desalination performance and antifouling properties of FO membranes, RSC Advances 6 (74) (2016) 70174–70185.
[114] M. Dadashi Firouzjaei, F. Akbari Afkhami, M. Rabbani Esfahani, C.H. Turner, S. Nejati, Experimental and molecular dynamics study on dye removal from water by a graphene oxide-copper-metal organic framework nanocomposite, Journal of Water Process Engineering 34 (2020) 101180, https://doi.org/10.1016/j.jwpe.2020.101180.
[115] M.D. Firouzjaei, A.A. Shamsabadi, M. Sharifian Gh, A. Rahimpour, M. Soroush, A novel nanocomposite with superior antibacterial activity: a silver-based metal organic framework embellished with graphene oxide, Advanced Materials Interfaces 5 (11) (2018) 1701365, https://doi.org/10.1002/admi.201701365.
[116] S.F. Seyedpour, A. Arabi Shamsabadi, S. Khoshhal Salestan, M. Dadashi Firouzjaei, M. Sharifian Gh, A. Rahimpour, F. Akbari Afkhami, M.R. Shirzad Kebria, M.A. Elliott, A. Tiraferri, M. Sangermano, M.R. Esfahani, M. Soroush, Tailoring the biocidal activity of novel silver-based metal azolate frameworks, ACS Sustainable Chemistry & Engineering 8 (20) (2020) 7588–7599, https://doi.org/10.1021/acssuschemeng.0c00201.
[117] R.E. Kesting, Semipermeable membranes of cellulose acetate for desalination in the process of reverse osmosis. I. Lyotropic swelling of secondary cellulose acetate, Journal of Applied Polymer Science 9 (2) (1965) 663–688.
[118] E. Curcio, E. Fontananova, G. Di Profio, E. Drioli, Influence of the structural properties of poly (vinylidene fluoride) membranes on the heterogeneous nucleation rate of protein crystals, The Journal of Physical Chemistry B 110 (25) (2006) 12438–12445.
[119] E. Fontananova, J.C. Jansen, A. Cristiano, E. Curcio, E. Drioli, Effect of additives in the casting solution on the formation of PVDF membranes, Desalination 192 (1–3) (2006) 190–197.
[120] J. Kong, K. Li, Preparation of PVDF hollow-fiber membranes via immersion precipitation, Journal of Applied Polymer Science 81 (7) (2001) 1643–1653.
[121] M. Tomaszewska, Preparation and properties of flat-sheet membranes from poly (vinylidene fluoride) for membrane distillation, Desalination 104 (1–2) (1996) 1–11.
[122] A. Karkooti, A.Z. Yazdi, P. Chen, M. McGregor, N. Nazemifard, M. Sadrzadeh, Development of advanced nanocomposite membranes using graphene nanoribbons and nanosheets for water treatment, Journal of Membrane Science 560 (2018) 97–107.
[123] B. Khorshidi, J. Hajinasiri, G. Ma, S. Bhattacharjee, M. Sadrzadeh, Thermally resistant and electrically conductive PES/ITO nanocomposite membrane, Journal of Membrane Science 500 (2016) 151–160.
[124] B. Khorshidi, S.A. Hosseini, G. Ma, M. McGregor, M. Sadrzadeh, Novel nanocomposite polyethersulfone-antimony tin oxide membrane with enhanced thermal, electrical and antifouling properties, Polymer 163 (2019) 48–56.
[125] M. Sadrzadeh, T. Mohammadi, Nanocomposite Membranes for Water and Gas Separation, Elsevier, 2019.

[126] J.B. Li, J.W. Zhu, M.S. Zheng, Morphologies and properties of poly (phthalazinone ether sulfone ketone) matrix ultrafiltration membranes with entrapped TiO2 nanoparticles, Journal of Applied Polymer Science 103 (6) (2007) 3623–3629.
[127] Y. Yang, H. Zhang, P. Wang, Q. Zheng, J. Li, The influence of nano-sized TiO2 fillers on the morphologies and properties of PSF UF membrane, Journal of Membrane Science 288 (1–2) (2007) 231–238.
[128] A. Mansourizadeh, A.F. Ismail, Effect of additives on the structure and performance of polysulfone hollow fiber membranes for CO2 absorption, Journal of Membrane Science 348 (1–2) (2010) 260–267.
[129] I. Wienk, R. Boom, M. Beerlage, A. Bulte, C. Smolders, H. Strathmann, Recent advances in the formation of phase inversion membranes made from amorphous or semi-crystalline polymers, Journal of Membrane Science 113 (2) (1996) 361–371.
[130] J.-H. Kim, K.-H. Lee, Effect of PEG additive on membrane formation by phase inversion, Journal of Membrane Science 138 (2) (1998) 153–163.
[131] D. Zhang, A. Karkooti, L. Liu, M. Sadrzadeh, T. Thundat, Y. Liu, R. Narain, Fabrication of antifouling and antibacterial polyethersulfone (PES)/cellulose nanocrystals (CNC) nanocomposite membranes, Journal of Membrane Science 549 (2018) 350–356.
[132] H. Caquineau, P. Menut, A. Deratani, C. Dupuy, Influence of the relative humidity on film formation by vapor induced phase separation, Polymer Engineering & Science 43 (4) (2003) 798–808, https://doi.org/10.1002/pen.10066.
[133] P. Aerts, I. Genné, R. Leysen, P. Jacobs, I. Vankelecom, The role of the nature of the casting substrate on the properties of membranes prepared via immersion precipitation, Journal of Membrane Science 283 (1–2) (2006) 320–327.
[134] X. Tian, Z. Wang, S. Zhao, S. Li, J. Wang, S. Wang, The influence of the nonsolvent intrusion through the casting film bottom surface on the macrovoid formation, Journal of Membrane Science 464 (2014) 8–19.
[135] X. Dong, T.J. Jeong, E. Kline, L. Banks, E. Grulke, T. Harris, I.C. Escobar, Eco-friendly solvents and their mixture for the fabrication of polysulfone ultrafiltration membranes: an investigation of doctor blade and slot die casting methods, Journal of Membrane Science 614 (2020) 118510, https://doi.org/10.1016/j.memsci.2020.118510.
[136] A.F. Ismail, A.R. Hassan, N.B. Cheer, Effect of shear rate on the performance of nanofiltration membrane for water desalination, Songklanakarin Journal of Science and Technology 24 (2002) 879–889.
[137] A. Asad, M. Rastgar, D. Sameoto, M. Sadrzadeh, Gravity assisted super high flux microfiltration polyamide-imide membranes for oil/water emulsion separation, Journal of Membrane Science 621 (2021) 119019.
[138] A. Asad, M. Sadrzadeh, D. Sameoto, Direct micropatterning of phase separation membranes using hydrogel soft lithography, Advanced Materials Technologies 4 (7) (2019) 1800384.
[139] A. Asad, M. Rastgar, H. Nazaripoor, M. Sadrzadeh, D. Sameoto, Durability and recoverability of soft lithographically patterned hydrogel molds for the formation of phase separation membranes, Micromachines 11 (1) (2020) 108.
[140] Y. Wang, Nondestructive creation of ordered nanopores by selective swelling of block copolymers: toward homoporous membranes, Accounts of Chemical Research 49 (7) (2016) 1401–1408.
[141] C.-Y. Yang, G.-D. Zhu, Z. Yi, Y. Zhou, C.-J. Gao, Critical contributions of additives on the fabrication of asymmetric isoporous membranes from block copolymers: a review, Chemical Engineering Journal 424 (2021) 128912, https://doi.org/10.1016/j.cej.2021.128912.
[142] K.-V. Peinemann, V. Abetz, P.F. Simon, Asymmetric superstructure formed in a block copolymer via phase separation, Nature Materials 6 (12) (2007) 992–996.
[143] S.P. Nunes, R. Sougrat, B. Hooghan, D.H. Anjum, A.R. Behzad, L. Zhao, N. Pradeep, I. Pinnau, U. Vainio, K.-V. Peinemann, Ultraporous films with uniform nanochannels by block copolymer micelles assembly, Macromolecules 43 (19) (2010) 8079–8085.
[144] M. Radjabian, J. Koll, K. Buhr, U. Vainio, C. Abetz, U.A. Handge, V. Abetz, Tailoring the morphology of self-assembled block copolymer hollow fiber membranes, Polymer 55 (13) (2014) 2986–2997.
[145] N. Bazrafshan, M. Dadashi Firouzjaei, M. Elliott, A. Moradkhani, A. Rahimpour, Preparation and modification of low-fouling ultrafiltration membranes for cheese whey treatment by membrane bioreactor, Case Studies in Chemical and Environmental Engineering 4 (2021) 100137, https://doi.org/10.1016/j.cscee.2021.100137.
[146] M. Bikel, P.Z. Çulfaz, L.A. Bolhuis-Versteeg, J.G. Pérez, R.G. Lammertink, M. Wessling, Polymeric microsieves via phase separation microfabrication: process and design optimization, Journal of Membrane Science 347 (1–2) (2010) 93–100.

[147] M. Bikel, I. Pünt, R.G. Lammertink, M. Wessling, Shrinkage effects during polymer phase separation on microfabricated molds, Journal of Membrane Science 347 (1−2) (2010) 141−149.
[148] L. Vogelaar, J.N. Barsema, C.J. van Rijn, W. Nijdam, M. Wessling, Phase separation micromolding—PSμM, Advanced Materials 15 (16) (2003) 1385−1389.
[149] M.A. Bikel, I.G. Punt, R.G. Lammertink, M. Wessling, Micropatterned polymer films by vapor-induced phase separation using permeable molds, ACS Applied Materials & Interfaces 1 (12) (2009) 2856−2861.
[150] L. Vogelaar, R.G. Lammertink, M. Wessling, Superhydrophobic surfaces having two-fold adjustable roughness prepared in a single step, Langmuir 22 (7) (2006) 3125−3130.
[151] Y.-J. Won, J. Lee, D.-C. Choi, H.R. Chae, I. Kim, C.-H. Lee, I.-C. Kim, Preparation and application of patterned membranes for wastewater treatment, Environmental Science & Technology 46 (20) (2012) 11021−11027.
[152] L. Vogelaar, R.G. Lammertink, J.N. Barsema, W. Nijdam, L.A. Bolhuis-Versteeg, C.J. Van Rijn, M. Wessling, Phase separation micromolding: a new generic approach for microstructuring various materials, Small 1 (6) (2005) 645−655.
[153] Y.-F. Gao, Y.-J. Huang, S.-Y. Xu, W.-J. Ouyang, Y.-B. Jiang, Ordered honeycomb microporous films from self-assembly of alkylated guanosine derivatives, Langmuir 27 (6) (2011) 2958−2964.
[154] S. Qin, H. Li, W.Z. Yuan, Y. Zhang, Fabrication of polymeric honeycomb microporous films: breath figures strategy and stabilization of water droplets by fluorinated diblock copolymer micelles, Journal of Materials Science 47 (19) (2012) 6862−6871.
[155] M. Srinivasarao, D. Collings, A. Philips, S. Patel, Three-dimensionally ordered array of air bubbles in a polymer film, Science 292 (5514) (2001) 79−83.
[156] G. Widawski, M. Rawiso, B. François, Self-organized honeycomb morphology of star-polymer polystyrene films, Nature 369 (6479) (1994) 387−389.
[157] H. Cong, J. Wang, B. Yu, J. Tang, Preparation of a highly permeable ordered porous microfiltration membrane of brominated poly (phenylene oxide) on an ice substrate by the breath figure method, Soft Matter 8 (34) (2012) 8835−8839.
[158] L.-S. Wan, J.-W. Li, B.-B. Ke, Z.-K. Xu, Ordered microporous membranes templated by breath figures for size-selective separation, Journal of the American Chemical Society 134 (1) (2012) 95−98.
[159] L.-S. Wan, L.-W. Zhu, Y. Ou, Z.-K. Xu, Multiple interfaces in self-assembled breath figures, Chemical Communications 50 (31) (2014) 4024−4039.

Abstract

Although nonsolvent-induced phase separation (NIPS) has been studied for more than 5 decades, it still draws much attention. Currently, membranes fabricated by phase inversion techniques, especially NIPS, are widely applied in many chemical industries, nanotechnology, and environmental separation operations. NIPS enables the fabrication of membranes with various characteristics and structures (i.e., porous or dense and symmetric or asymmetric). Several factors affect membrane fabrication by NIPS method, including polymer type and concentration, solvent and nonsolvent system types, composition or additives of the polymer casting solution, and film casting conditions. In this chapter, we investigate the influence of these factors on the structural characteristics of membranes fabricated via NIPS technique. Also, we discuss deeply the membrane formation mechanism, phase diagram, thermodynamic, and kinetic aspects of the phase inversion process induced by nonsolvents.

Keywords:

Delayed and spontaneous demixing; Kinetic hindrance; Membrane; Microfiltration; Nonsolvent-induced phase separation; Ternary phase diagram; Thermodynamic enhancement; Ultrafiltration.